Journal of Hydrology 598 (2021) 126383

Contents lists available at ScienceDirect

Journal of Hydrology

journal homepage: www.elsevier.com/locate/jhydrol

Research papers

Characterizing natural drivers of water-induced disasters in a rain-fed watershed: Hydro-climatic extremes in the Extended East Rapti Watershed, Nepal

Vishnu Prasad Pandey [a,b,*], Dibesh Shrestha [a,c], Mina Adhikari [d]

[a] International Water Management Institute, Nepal Office, Lalitpur, Nepal
[b] Department of Civil Engineering, Pulchowk Campus, Institute of Engineering, Tribhuvan University, Lalitpur, Nepal
[c] Nepal Development Research Institute, Lalitpur, Nepal
[d] Nepal Water Conservation Foundation for Academic Research, Kathmandu, Nepal

ARTICLE INFO

Keywords:
Climate change
Climate extremes
East Rapti
Hydrological extremes
Water induced disasters

ABSTRACT

Extreme climatic and hydrological events result in water-induced disasters and associated loss and damage of lives, livelihoods, and properties. It is related with various climatic, topographical, and anthropogenic factors, and therefore, expected to vary widely across the watersheds. This study characterized historical and projected future trends in climatic extremes, their spatial variations, hydrological extremes, and linkage between hydro-climatic extremes for a rain-fed *Extended East Rapti (EER)* watershed in Central-Southern Nepal. The watershed feeds into *the Ganges* in the South Asia through the *Gandaki* river. A set of 14 climate extreme indices, seven related to precipitation and seven to temperature, and eight hydrological indices were selected to characterize the extremes. Climatic and hydrological extreme indices were computed using RClimDex and IHA (Indicators for Hydrological Alteration) tools, respectively. Trends were calculated using the Modified Mann-Kendall test and Sens's slope estimator. Relationship between hydrological and climatic extremes was evaluated by checking dates for rainfall extreme, hydrological extreme, and reported cases of flooding during that period. Results showed increasing trends in both precipitation and temperature extremes for the historical period (1980–2005) with a rate of 10–35% increase in RX1day (monthly maximum 1-day precipitation), 10–50% increase in R95p (very wet days precipitation amount) and 15–60% increase in warm nights from the base period until the mid-century. Hydrological alterations in terms of increasing extremes are also clearly visible in maximum flows, minimum flows as well as the shift in the day of maximum flow. Since, hydro-climatic extremes bear a direct relationship, future hydrological extremes, primarily floods, are expected to increase in future.

1. Introduction

Nepal is one of the most disaster-prone country in the world ranking 4th, 11th, and 30th with regards to climate-related hazards, earthquakes, and flood hazards, respectively (MoHA/GoN, 2017). Nepal's unique geo-physical setting, topographical diversity, ecological variability (from sub-tropical to arctic within just a few hundred kilometres), varied climate and natural hazards has made it vulnerable to natural disasters in general, and climate-related disasters in particular. The weather/climate-related disasters include both geo-physical events (e.g., earthquakes, glacial lake outburst floods, landslides) and hydro-meteorological events (e.g., floods (both flash and riverine) and droughts). Hydro-meteorological events in this study are defined as "Water-Induced Disasters (WIDs)".

Water-induced disasters (WIDs) are recurring events which result in significant human sufferings every year (MoHA/GoN, 2017). An estimated direct costs related to WIDs in Nepal during 1980 and 2000 ranged between 1.5 and 2.0% of gross domestic product (GDP); a figure that has gone up as high as 5% (MoSTE, 2014). The government data reveals the most observable and direct impact on the communities whose lives and livelihood are connected with their riverine ecosystem. For example, from 2011 to 2014, 395 persons died due to floods; 376 due to landslides; 95 due to heavy rainfall (MoHA/GoN, 2015). About an equal number of people were also missing and presumed dead from these WIDs. In all these instances of disasters, the section of the society that is oftentimes the most affected is the women, children, and the

* Corresponding author.
E-mail addresses: vishnu.pandey@pcampus.edu.np (V.P. Pandey), dibeshshrestha@live.com (D. Shrestha).

https://doi.org/10.1016/j.jhydrol.2021.126383

Available online 29 April 2021

elderly. For instance, during the Koshi River Flood of 2008, of the 4,634 families registered in various camps in Sunsari district alone, there were 333 pregnant women, 200 post-partum mothers, 131 disabled men and women, and 581 elderly people (OCHA, 2008).

Social, development and natural factors may contribute to increase vulnerability of populations to WIDs. Factors related to weather or climatic change are considered as natural roots. Climate change/variability is exacerbating weather anomalies, droughts, floods, and other climate-related phenomena across the globe (Senevirante et al., 2012). For example, the onset and end of monsoon in Nepal are changing noticeably over the years (Rijal, 2015). Although the total annual rainfall remains more or less the same, high-intensity-short-duration rainfall, ones that are likely to result in disasters, have increased noticeably (Pokharel and Hallett, 2015; Talchabhadel et al., 2018). In the hilly areas, such events trigger various forms of WID, including erosion and landslides; in the valleys and the flatlands these cause severe flooding. These events adversely affect the lives and the livelihoods of local communities (HI-AWARE, 2017; ICIMOD, 2017). This abundance of water is concentrated entirely during the four monsoon months (June-September) and the rest of the year these regions are practically dry. Climate change/variability in the recent years has also increased the occurrence of dryness during part of the wet as well as the dry season (Senevirante et al., 2012).

Nepal has made a notable progress in climate action and disaster risk management over the decades with a number of legal and institutional reforms to address the worsening situation of populations exposed to the cumulative risk of natural hazards and climate change. However, national and local developments remain disjointed to risk-informed evidence-based planning. The policy and actions on climate and disaster continue to operate in silos. Further, there are limited empirical evidence regarding disaster and climate risk mitigation based on long-term scenario analysis using hydro-climatic extremes. In this context, it is urgent to assess the hydro-climatic extremes scenarios for forecasting future conditions and their implications on disaster and climate risk mitigation. It is imperative to understand magnitude, frequency and timing of hydro-climatic extremes, their trends over historical and future periods, and discuss their implications on various aspects of society and ecosystem so that we can get prepared better to minimize the risks and losses from WIDs. The hydro-climatic extremes can be characterized in the form of precipitation extremes, temperature extremes, and hydrologic extremes.

Characteristics of climatic extremes, including frequency, amplitude and persistence can be described with a set of indices defined by Expert Team on Climate Change Detection and Indices (ETCCDI) (WMO, 2009) derived from daily time series of precipitation and temperature (Table 2). The R-based tools such as RClimDex (Zhang et al., 2018) are available to calculate the relevant climate indices. RClimDex has been used by many studies over the years (e.g., Alexander et al., 2006; Donat et al., 2013; Islam, 2009; Kiktev et al., 2003; Shrestha et al., 2017). Though both parametric and non-parametric tests can be used for detection and attribution of trends, non-parametric tests are preferred as they are distribution-free tests. One of the widely used non-parametric tests for detecting a trend in hydro-climatic time series is the Mann–Kendall (Kendall, 1975; Khatiwada et al., 2016; Mann, 1945). Understanding trends in climatic extremes in both historical and future climate series are important for informed climate-resilient development planning and decision-making.

Observed climatic data for historical trends are readily available from the hydro-met department in a country. However, future climate of an area is projected using General Circulation Models (GCMs) or Regional Circulation Models (RCMs). RCMs are widely used for the climate impact studies (e.g., Berckmans et al., 2019; Gaur et al., 2020; Gutowski et al, 2020; Jacob et al., 2020; Pandey et al., 2019; Stefanidis et al., 2020) due to its higher resolution and better capturing of regional conditions. RCM projections are further corrected for biases to make them usable for a watershed of interest. Various methods are available for bias correction, and quantile mapping (Gudmundsson et al., 2012) is applicable in most of the cases (Enayati et al., 2020; Pandey et al., 2019, 2020a).

Trends in various aspects of streamflow, one of the important hydrological components affected by both climatic and non-climatic factors, can be analyzed by various statistical approaches as described in literatures (e. g., Dery et al., 2016; Kundzewicz et al., 2015; Panda et al., 2013). Some studies have even demonstrated statistically significant links of streamflow trends with temperature or precipitation (Bates et al., 2008). Indicators of Hydrologic Alteration (IHA) (Richter et al., 1996, 1997) is a tool, comprising of 32 parameters, that characterizes hydrological variability and represents various aspects of the hydrological extremes (Bharati et al., 2016).

There are several studies that assesses climate change impacts in water availability in Nepal (e.g. Devkota and Gyawali, 2015; Lamichhane and Shakya, 2019; Pandey et al., 2019, 2020a). However, studies focusing on climate projection using RCMs and the most recent representative concentration pathways (RCPs) scenarios are limited in Central-Southern Nepal in general, and *Extended East Rapti (EER)* watershed in particular. Furthermore, studies focusing on both historical and future climatic extremes as well as hydrological extremes are limited. This study therefore aims to unpack hydro-climatic extremes in the *EER* watershed located in Central-Southern Nepal that feeds to *Gandaki* (Fig. 1) and then to the Ganges, by answering following research questions: i) What are historical and future trends in climatic extremes and how do they vary spatially? ii) What are historical trends in hydrological extremes? iii) What are the links between hydro-climatic extremes and associated WIDs?

2. Description of the study area

The EER watershed extends between 84.148°E to 85.206°E longitude and 27.353°N to 27.783°N latitude in the Bagmati Province in Nepal (Fig. 1). As water from outlet of Kulekhani dam is diverted into the East Rapti watershed, the very first case of inter-basin water transfer in Nepal, Kulekhani watershed above the dam is practically the headwater of East Rapti, even though it is within different hydrological boundary. Therefore, it is also considered as watershed area of East Rapti even though hydrological boundary is different, and therefore, defined as EER watershed in this study.

The watershed area delineated above the confluence with the Gandaki river and including Kulekhani watershed is 3,202 km^2. The watershed has dominance of forest cover (65.5%) and agricultural area (28.8%) (as per data from ICIMOD, 2010), extends from an elevation of 136 to 2,579 m above the mean sea level (masl), and hosts 2.9% of Nepal's population (as per 2011 census). It extends over two districts, 15 (rural) municipalities, one wildlife reserve, and one national park. There are many water infrastructures in the watershed. The numbers of irrigation projects alone are over 70, with varying command areas, as per the National Irrigation Master Plan (draft) database developed by Department of Water Resources and Irrigation (DWRI).

There are three hydrological and eight meteorological stations in the watershed (Fig. 1). Climate in the EER watershed is characterized as humid sub-tropical. Average annual rainfall in the EER watershed based on data at eight meteorological stations vary from 1,750 mm (at Daman) to 2,365 mm (at Hetauda), but have strong seasonality at all the stations, with rainy season (JJAS) receiving about 80% of total annual rainfall. Average monthly maximum temperature (Tmax) in the EER watershed varies from 22.0 °C in January to 35.9 °C in June, whereas average monthly minimum temperature (Tmin) varies from 7.7 °C in January to 25.4 °C in August. In terms of water availability, an average annual discharge at the EER outlet is 135 m^3/s (or 4,291 million-cubic-meters-a-year) (Ray, 2020).

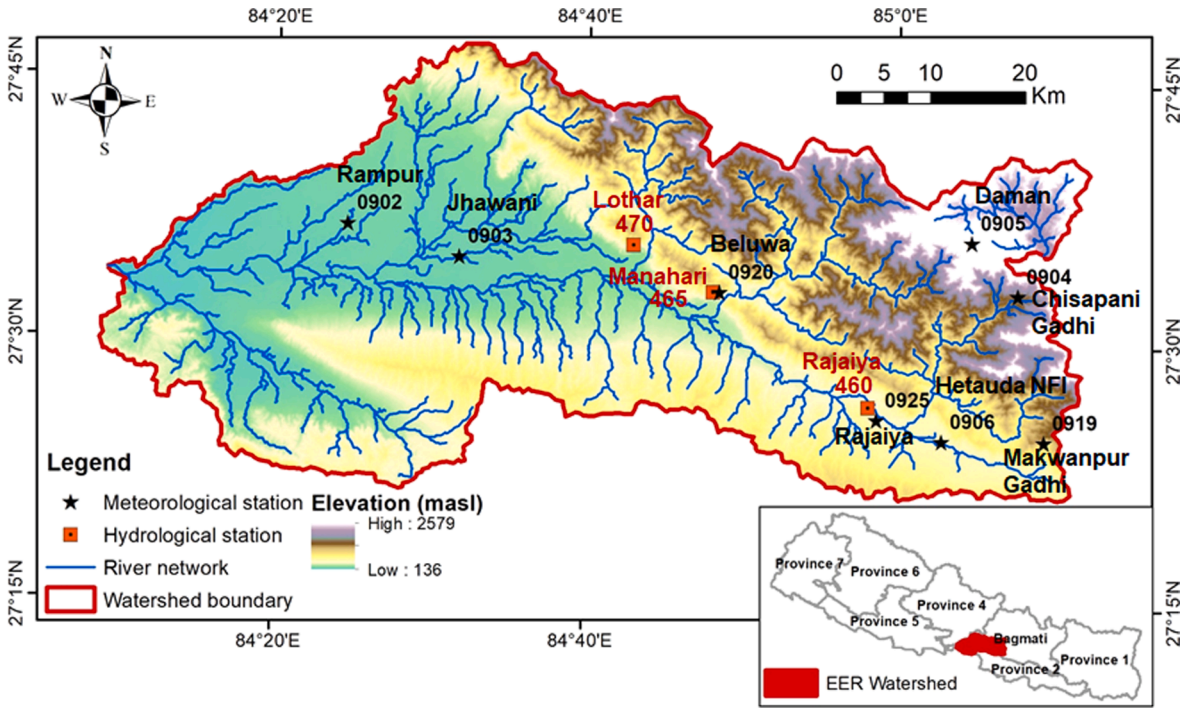

Fig. 1. Location and associated details of the EER watershed, Nepal.

3. Methodology and data

The overall methodological framework for this study consists of collecting and pre-processing observed and projected future climatic data, identifying and selecting suitable set of climatic extremes, quantifying the climatic extremes for historical and future time periods, characterizing hydrological extremes, and then identifying the links between climatic extremes and hydrologic extremes. They are described in the following sub-sections.

3.1. Data collection and pre-processing

3.1.1. Observed historical data

Description of various types of data used in this research is provided in Table 1 along with their sources. There are eight rainfall stations and three discharge gauging stations in the watershed. Daily time series of precipitation and temperature (both maximum and minimum) data were collected from Department of Hydrology and Meteorology (DHM), the Government of Nepal. The quality of observed data was assessed based on extent and concentration of missing values, data reading to ensure reliability of recorded values, plotting of hyetographs of various temporal scale (e.g., daily, monthly, annual), and plotting of mass curves.

Missing daily precipitation data was imputed using Inverse Weighted Distance (IDW) interpolation at daily scale with power factor of 2. In case of temperature, missing values were estimated using laps rate from the nearest neighbour. Lapse rate used for maximum and minimum temperature were the drop of 5.9 °C and 4.4 °C per 1000 m altitude respectively as shown in Fig. 2. They were computed from annual average values from three stations namely, Rampur (Index: 902), Daman (Index: 905), and Hetauda (Index: 906). Finally, appropriate time period for data analysis as mentioned in Table 1 was selected based on adequacy of data availability, quality, and spatial coverage within the EER watershed.

Table 1
Description of various types of data used in this study.

Data [Unit]	Data Type	Description/ Properties	Data Source	Resolution [Time frame]
Historical Rainfall [mm]	Time series	Daily observed precipitation	DHM, Nepal	8 stations [1980–2005]
Historical maximum and minimum temperatures [°C]	Time series	Daily observed maximum and minimum temperatures	DHM, Nepal	3 stations [1980–2005]
Regional Climate Model (RCM) Precipitation [mm] and Temperatures [°C]	Time series extracted from spatial grids	Daily projected values in grids, available to download as *netcdf* format.	19 RCMs from CORDEX-SA (Annex-A)	0.44° x 0.44° [1981–2095]
Historical streamflow [m^3/s]	Time series	Daily observed streamflow	DHM, Nepal	3 stations [1980–2005]

3.1.2. Future climate data

Nineteen RCMs available in Coordinated Regional Downscaling Experiment for South Asia (CORDEX-SA) platform were downloaded, pre-processed, and evaluated as discussed in Dhaubanjar et al. (2020). Annex-A provides characteristics of the RCMs. We derived the consensus climate future for the EER watershed in Central Nepal (84–85.5°E longitudes and 27-28°N latitudes) from the 19 RCMs using the Australian Climate Futures Framework (Clarke et al., 2011; Whetton et al., 2012). Projected changes in annual temperature and precipitation were classified into qualitative categories of changes to generate a climate future matrix (CFM) as shown in Fig. 3. Three future periods were investigated: near-future (NF; 2021–2045), mid-future (MF; 2046–2070), and far-future (FF; 2071–2095). The baseline considered was 1980–2005. Considering two representative concentration pathways (RCPs) scenarios (RCP 4.5 and 8.5) and three future periods, six CFMs were developed for the ERR watershed. For each of these six CFMs, the RCMs that represent the consensus case (i.e., the cell in the matrix with the maximum number of RCM model projections for a combination of particular precipitation and temperature class) were identified and selected.

Table 2
Climatic extremes indices considered in this study.

Name of Index / Notation / Units	Description	Estimation Method
Temperature related indices		
Maximum of daily maximum temperature (TXx) [°C]	Monthly/ Annual maximum value of daily maximum temperature	Let TX_x be the daily maximum temperatures in month$k$, period$j$. The maximum daily maximum temperature each month is then$TX_{x_{kj}} = max(TX_{x_{kj}})$
Maximum of daily minimum temperature (TNx) [°C]	Monthly /Annual maximum value of daily minimum temperature	Let TN_x be the daily minimum temperatures in month k, period$j$. The maximum daily minimum temperature each month is then$TN_{x_{kj}} = max(TN_{x_{kj}})$
Minimum of daily maximum temperature (TXn) [°C]	Monthly/ Annual minimum value of daily maximum temperature	Let TX_n be the daily maximum temperatures in month k, period$j$. The minimum daily maximum temperature each month is then$TX_{n_{kj}} = min(TX_{n_{kj}})$
Minimum of daily minimum temperature (TNn) [°C]	Monthly /Annual minimum value of daily minimum temperature	Let TN_n be the daily minimum temperatures in month k, period j. The minimum daily minimum temperature each month is then$TN_{n_{kj}} = min(TN_{n_{kj}})$
Warm days (TX90p) [%]	Percentage of days with TX > 90th percentile	Let TX_{ij} be the daily maximum temperature on day i in period$j$ and let $TX_{in}90$ be the calendar day 90th percentile centered on a 5-day window. The percentage of time is determined where $TX_{ij} > TX_{in}90$
Warm nights (TN90p) [%]	Percentage of days when TN > 90th percentile	Let TN_{ij} be the daily minimum temperature on day i in period$j$ and let $TN_{in}90$ be the calendar day 90th percentile centred on a 5-day window . The percentage of time is determined where $TN_{ij} > TN_{in}90$
Warm Spell Duration index (WSDI) [days]	Annual count of days with at least 6 consecutive days with TX > 90th percentile	Let TX_{ij} be the daily maximum temperature on day i in period$j$ and let $TX_{in}90$ be the calendar day 90th percentile centered on a 5-day window. Then the number of days per period is summed where, in intervals of at least 6 consecutive days$TX_{ij} > TX_{in}90$
Precipitation related indices		
Consecutive dry days (CDD) [days]	Maximum number of consecutive days with daily precipitation less than 1 mm	Let RR_{ij}be the daily precipitation amount on day i in period$j$. Count the largest number of consecutive days where $RR_{ij} < 1mm$
Consecutive wet days (CWD) [days]	Maximum number of consecutive days with daily precipitation ≥ 1 mm	Let RR_{ij} be the daily precipitation amount on day i in period$j$. Count the largest number of consecutive days where $RR_{ij} \geq 1mm$
Annual total wet-day precipitation (PRCPTOT) [mm]	Annual total precipitation in wet days (Daily precipitation ≥ 1 mm)	Let RR_{ij}be the daily precipitation amount on day i in period$j$. If Irepresents the number of days in j, then $PRCPTOT_j = \sum_{i=1}^{I} RR_{ij}$
Very wet days (R95p) [mm]	Annual total PRCP when RR > 95p	Let RR_{wj} be the daily precipitation amount on a wet day w ($RR \geq 1.0\ mm$) in period j and let $RR_{wn}95$ be the 95th percentile of precipitation on wet days in the base period. If Wrepresents the number of wet days in the period, then$R95p_j = \sum_{w=1}^{W} RR_{wj}$ where $RR_{wj} > RR_{wn}95$
Annual / Monthly maximum 1-day precipitation (RX1day) [mm]	Most intense rainfall event in 1-day for a given month / year	Let RR_{ij} be the daily precipitation amount on day i in period$j$. Then maximum 1-day values for period j are $RX1day_j = max(RR_{ij})$
Annual / Monthly maximum consecutive 5-day precipitation (RX5day) [mm]	Most intense rainfall event in 5 consecutive days for a given month / year	Let RR_{kj} be the precipitation amount for the 5-day interval ending k, period$j$. Then maximum 5-day values for period$j$ are$RX5day_j = max(RR_{kj})$
Heavy rainfall days (R20) [days]	Annual count of days when precipitation > 20 mm	Let RR_{ij} be the daily precipitation amount on day i in period j. Count the number of days where $RR_{ij} \geq 20mm$

Notes: P is precipitation; T is temperature; RH is relative humidity; Q is discharge.

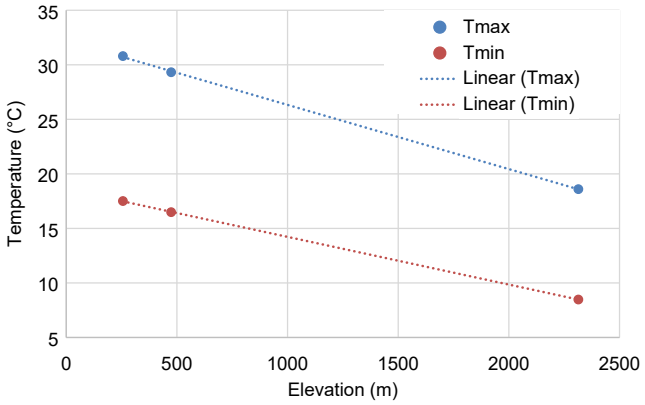

Fig. 2. Lapse rate used for imputing daily maximum and minimum temperature.

The future climate data at the meteorological stations were then bias-corrected using empirical quantile mapping (QM) method (Gudmundsson et al., 2012; Teutschbein and Seibert, 2012), implemented in R using a qmap package (Gudmundsson et al., 2012). QM corrects quantiles of RCM data to match with that of observed ones. Its basic structure is given by:

$$X^{corr}_{future,t} = inv.ecdf^{obs}_{baseline}\left(ecdf^{RCM}_{baseline}\left(X^{RCM}_{future,t}\right)\right)$$

where, *ecdf* is empirical cumulative distribution function for the reference time period, $X^{RCM}_{future,t}$ is the raw RCM (projected value) in future at time t, $ecdf^{RCM}_{baseline}$ is empirical cumulative distribution function of RCM for baseline time period, and $inv.ecdf^{obs}_{baseline}$ is the inverse empirical cumulative distribution function of observation for baseline time period. $X^{corr}_{future,t}$ is the corrected estimate of $X^{RCM}_{future,t}$. The ecdf and inverse ecdf functions were derived for each of the months. For the RCM values in future period which lies beyond the range of values in the baseline period, the corrected estimate was obtained by multiplying $X^{RCM}_{future,t}$ with the ratio of maximum (or minimum) of observation to maximum (or minimum) of RCM values in baseline period for precipitation. In case of the temperature, corrected estimate was obtained by addition of difference between maximum (or minimum) of observation and maximum (or minimum) of RCM values. If the frequency of dry days in the baseline period in RCM data is greater than frequency of dry days in the observed data, correction was made for the extra dry days because any dry day is mapped to a precipitation day leading to wet bias (Themeßl et al., 2012). This was achieved by 'Frequency Adaptation (FA) (Themeßl et al., 2012)', in which only the fraction, ΔP_0, of such dry-day cases with probability $P_0$are corrected randomly by uniformly sampling a number between zero precipitation and the precipitation amount of $inv.ecdf^{obs}_{baseline,t}(ecdf^{RCM}_{baseline,t}(0))$.

$$\Delta P_0 = \frac{ecdf^{RCM}_{baseline}(0) - ecdf^{obs}_{baseline}(0)}{ecdf^{RCM}_{baseline}(0)}$$

A multi-model ensemble of the bias corrected times series for the

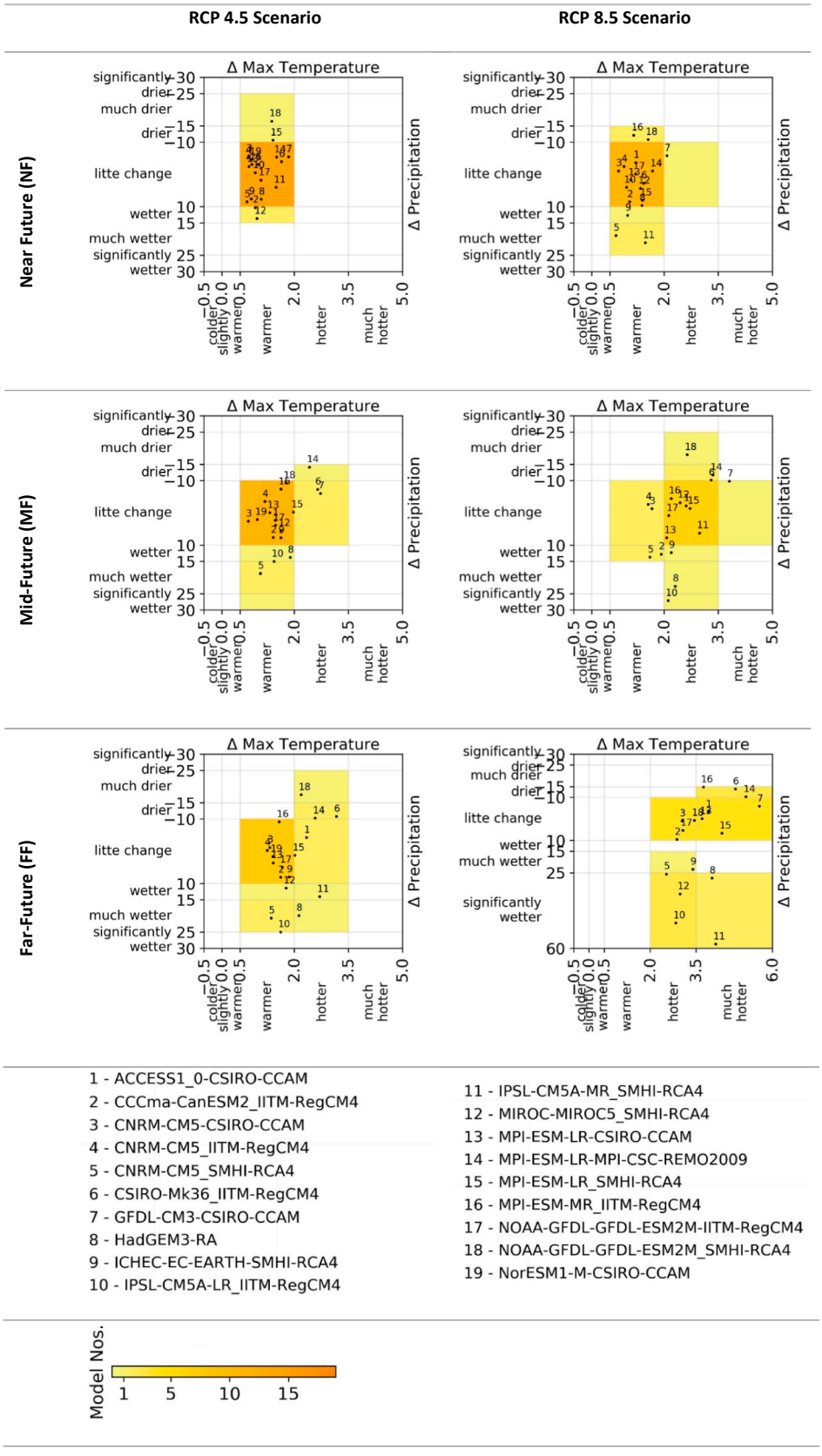

Fig. 3. Climate future matrices for the Extended East Rapti (EER) watershed. (Notes: Changes in precipitation are in percentage and changes in temperature are in °C. NF, MF and FF represent near-future (2021–2045), mid-future (2046–2070) and far-future (2071–2095). Number from 1 to 19 refers to the RCM identification number in Annex-A).

RCMs in the consensus case for each of the six climate futures were then generated. The projected changes in future climate extremes were analysed based on the ensemble.

The RCMs considered for generating ensemble varies across the future periods as well as scenarios considered as shown in the CFMs in Fig. 3 (please refer Annex B for the list of RCMs). The colour scale in the figure shows the number of RCMs in each of cells in the matrix belonging to particular combination of temperature and precipitation changes. For all six cases, model consensus on changes in average annual precipitation are in "Little change (-10% to + 10%)" class. In case of temperature changes, in RCP 4.5 scenario, consensus among models are in "warmer (0.5 °C to 2.0 °C)" category. However, in RCP 8.5 scenario for MF and FF, models show consensus on "hotter (2.0 °C to 3.5 °C)" class though for NF, most of models fall in "warmer" category. In RCP 8.5 scenario for FF, four models fall in each category for "hotter" and "much hotter" cases. Since, spread of temperature changes among models on "hotter" case is less than "much hotter" case, we choose the former one. From the six CFMs, we observed that EER watershed is projected to be warmer to hotter in future while there is "little change" in precipitation. Since, maximum temperature highly correlates with the minimum temperature; we used daily maximum temperature for deriving the CFMs.

3.2. Identifying and quantifying climatic extremes

A core set of 29 ETCCDI climate indices derived from daily time series of precipitation and temperature were calculated using the R-based RClimdDex package (Zhang et al., 2018). They are widely used for analyzing global changes in extremes in observational records and future climate change projection (Sillmann et al., 2013a, 2013b). Out of the 29 indices, we selected 14 climate extreme indices (7 related to precipitation and 7 related to temperature) as listed in Table 2, from careful review of literature and discussion with experts. Selection was mainly focused on how these extreme conditions, especially the precipitation extremes, influence hydrology of the study area. RX1day and RX5day represents conditions for high antecedent soil moisture that may lead to floods and landslides in the mountainous catchment. Wet days precipitation (R95p), is also similar indicator of wet extreme conditions. CDD is especially important for dry spells affecting reduction in water availability. CWD on other hand is also both important for water availability. R20 can be related to frequency of high flow events. And PRCPTOT generally indicates overall wet and dry conditions. Long warm spells, which is indicated by WSDI, can cause conditions favourable for reduction in water availability like in soil moisture storage due to increase in evapotranspiration. Temperature indices like TXx, TNx, TXn, TNn, TX90p and TN90p were selected as they are generally accepted indicators used for climate extreme detection. The indices were calculated for both historical and projected future climate series. Results are discussed in terms of amount of trend, their direction and statistical significant. Furthermore, changes in these extreme indices in future period were also assessed.

Trends in the climate extreme indices were analysed using non-parametric Modified Mann-Kendall test (M−MKT) (Hamed and Rao, 1998), Sen's slope estimator (Hirsch et al., 1982), and Spearman's Rho (Lehmann, 1975) tests. The M−MKT accounts for the presence of autocorrelation in the data in addition to other advantages from original MK test. Once presence of trend is confirmed from M−MKT, magnitude of trend was estimated using Sen's slope estimator. The significance of the detected trend was evaluated using Spearman's Rho test. Spatial variation of trends in precipitation and temperature extremes across the EER watershed was visualized and analysed using geo-spatial maps prepared in ArcGIS. Technical details on computation of M−MKT is provided in Hamed and Rao (1998), which is a modified version of non-parametric rank-based MKT (Kendall, 1975; Mann, 1945). In MKT, the null hypothesis H_0 is that data are independent and randomly placed with no serial correlation structure among the observations. Similarly, literatures like Lehmann (1975) and Sneyers (1990) provide technical details related to the Spearman's Rho test and Sen (1968) provides details on Sen's slope estimator.

3.3. Identifying and quantifying hydrological extremes

Daily streamflow time series observed at the three stations for the period of 1980–2005, located in the EER watershed (Fig. 1), and having characteristics as detailed in Table 1, were collected from DHM. These three sub-watersheds cover approximately 32.5% of the EER watershed. The streamflow data were checked for quality, including consistency before using for the analysis. Indicators of Hydrologic Alterations (IHA), a tool developed by Richter et al. (1996) and detailed in Mathews and Richter (2007) was used for characterizing hydrological extremes. IHA uses a nonparametric range of variability (RVA) approach (Richter et al., 1997) to characterize alterations in inter- and intra-annual variation in river flow. The analysis was based on observed data and no hydrological simulations were involved with it. RVA is based upon comprehensive statistical characterization of the temporal variability in hydrologic regime quantifying the degree of alteration of 33 ecologically relevant hydrologic parameters (Table 3) that describe crucial relationships between flow and ecological functions (Mathews and Richter, 2007). The indicators are divided into five groups representing different characteristics of flow regimes as shown in Table 3. These groups are (a) magnitude of monthly water condition, (b) magnitude and duration of

Table 3
IHA indicators for hydrological extremes – groups, regime characteristics, and parameters.

IHA statistics group	Regime characteristics	Hydrologic parameters
Group 1: Magnitude of monthly water condition	Magnitude, Timing	Mean value for each calendar month (Total 12 parameters)
Group 2: Magnitude and duration of annual extreme water condition	Magnitude, Duration	Annual minima, 1-day mean Annual minima, 3-day means Annual minima, 7-day means Annual minima, 30-day means Annual minima, 90-day means Annual maxima, 1-day mean (Daily peak flood) Annual maxima, 3-day means Annual maxima, 7-day means (7-day maximum flood) Annual maxima, 30-day means Annual maxima, 90-day means Number of zero-flow days Base flow index: 7-day minimum flow/mean flow for year (Total 12 parameters)
Group 3: Timing of annual extreme water conditions	Timing	Julian date of each annual 1-day maximum Julian date of each annual 1-day minimum (Total 2 parameters)
Group 4: Frequency and duration of high and low pulses	Magnitude, Frequency, Duration	Number of low pulses within each water year Mean or median duration of low pulses (days) Number of high pulses within each water year Mean or median duration of high pulses (days) (Total 4 parameters)
Group 5: Rate and frequency of water condition changes	Frequency, Rate of change	Rise rates: Mean or median of all positive differences between consecutive daily values Fall rates: Mean or median of all negative differences between consecutive daily values Number of hydrologic reversals (Total 3 parameters)

annual extreme water condition, (c) timing of annual extreme water conditions, (d) frequency and duration of high and low pulses and (e) rate and frequency of water condition changes. Importance of these groups is described in detail in Richter et al. (1996) and The Nature Conservancy (2009). Computation and further details in the IHA can be found in The Nature Conservancy (2009) and Mathews and Richter (2007). Geomorphic and ecologic implication of the IHA parameters is described in detail in Graf (2006).

In RVA analysis for this study, we used three different categories of equal size for each of IHA parameter, the boundaries of which are based on percentiles. Lowest category contains all values less than or equal to the 33rd percentile; the middle category contains all values falling in the range of the 34th to 67th percentiles; and the highest category contains all values greater than the 67th percentile. We divided the base period into pre-1990 (1980–1990) and post-1990 (1991–2005) periods, as change point was detected by Pandey et al. (2020b) in 1990, and then computed the hydrologic alteration between these periods. The Hydrologic Alteration (HA) factor was then calculated for each of the three categories which is basically the difference between observed frequency and expected frequency divided by the expected frequency of the parameter. The expected frequency is the frequency with which the post-1990 values of the IHA parameters should fall within each category defined in pre-1990 period. These alterations have directions, positive and negative. Position alteration means the increase in frequency from the pre-1990 to the post-1990 period while negative alteration mean decrease. Degree of alteration are also divided into three classes namely, low, median and high. If absolute value of alteration ranges from 0 to 33% then changes are of low degree while if it is between 34 and 67% then degree of alteration is of middle category. Alteration beyond 67% is categorized as high alteration.

4. Results and discussion

4.1. Comparison of RCM-based extreme indices with observations

Comparison of the RCM-based extreme indices and monthly precipitation / temperature (maximum) against observations for the baseline period (1980–2005) are made in order to investigate if the modelled values from RCMs are consistent with the observations. Results are depicted in percentile-based plots in Fig. 4. It shows values of mean areal extreme precipitation and temperature indices at percentiles from 1 to 99. Range of 19 RCMs along with the multi-model mean value before and after bias correction against observation are shown along with observation. Ensemble spread of RCMs is large, which suggests that RCMs are fairly unable to capture the extremes, even though ensemble mean in some cases is closer to the observation as in CWD and TXx. This can simply be due to the fact that RCMs are forced by parent GCMs that may not able to represent the variation of climate dynamics in mountains. In case of indices like PRECTOT and R95p, ensemble mean shows overestimation of the extremes. RCMs model spread is higher at higher percentiles, and RX1day and RX5day rainfall are underestimated as shown by ensemble mean. This can be due to limitations of RCMs to describe heavy precipitation processes. Absolute-value based temperature indices as TNx, TXn and TNn are underestimated by RCMs, though count based indices like TX90p and TN90p are in agreement with observation. Wide spread of RCMs also can be observed in monthly precipitation and temperature values. In general, RCMs are underestimating the precipitation in monsoon (JJAS) months and overestimating in dryer months. Temperature (here, daily maximum) is also underestimated.

After bias correction using quantile mapping, spread of RCMs are

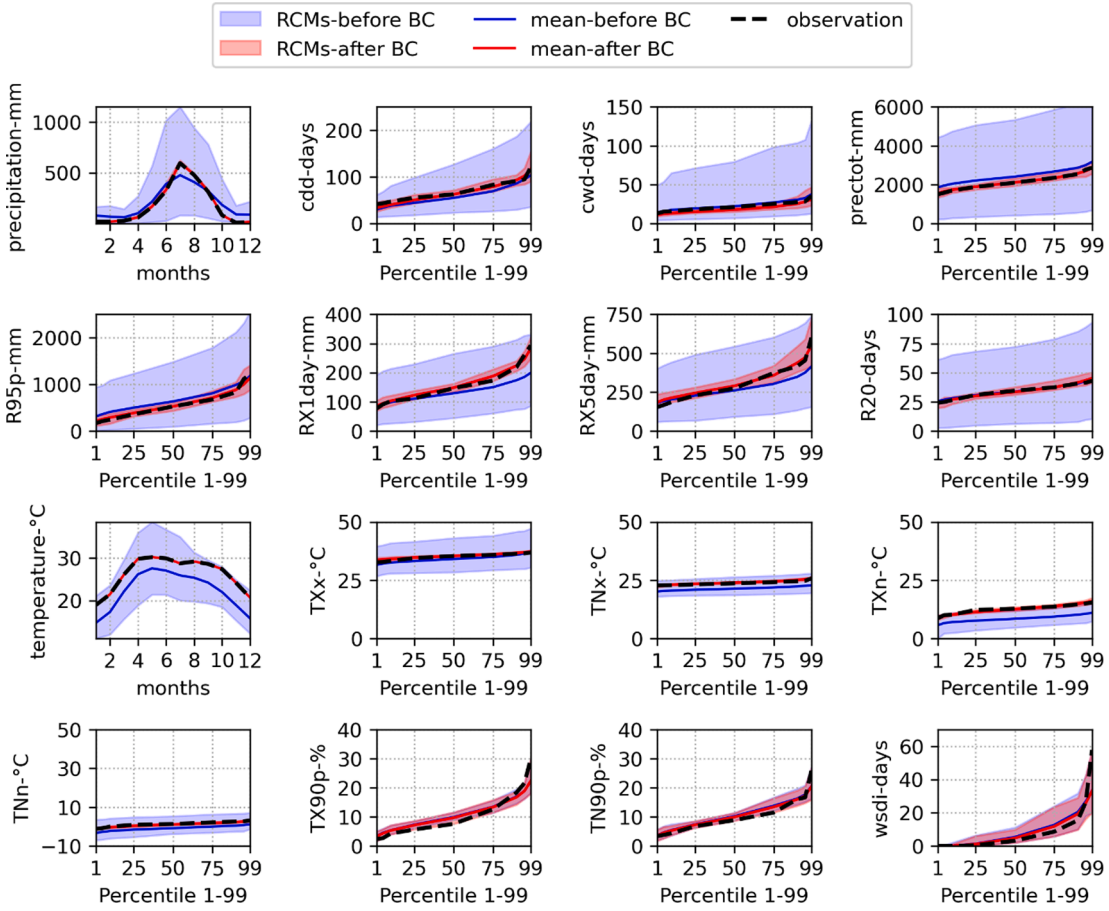

Fig. 4. Spread of extreme indices from RCMs in historical period 1980–2005 before and after bias correction against observation at different percentiles.

narrowed down and they match closely with observation. Though in few cases like wsdi and TX90p, bias correction is not effective especially at higher percentiles. Differences in the distribution of extreme indices between observation and RCMs were examined using Kolmogorov-Smirnov Test (2-sample) at level of significance $\alpha = 0.05$ with the null hypotheses that they come from same distribution. Distance between distributions is given by D statistics, with higher D indicating more differences. The results are shown in Fig. 5(a). RCM-based indices, before bias correction, have their distribution significantly different than of the observed distribution (orange-red colour grid boxes), suggesting that RCMs generally lack fidelity to capture small scale extreme phenomenon. This has been addressed after bias correction (blue coloured grid boxes).

With regards to the trends, most of the projected trends (raw RCMs) for temperature-based indices like TX90p and TN90p agree with the increasing observed trends during the baseline period with statistically significant slopes at $\alpha = 0.05$. The results are similar after bias correction as shown in Fig. 5(b). In contrast, for indices like TNn and TXn, observed trends are decreasing (not significant) while most of the raw and bias corrected RCMs show increasing trends (also not significant). For indices TXx and TNx, observed trends are increasing (not significant) and so as for most of RCMs before and after bias correction (not significant). In case of precipitation-based indices, increasing trend with statistically significant slopes at $\alpha = 0.05$ are observed for prectot, R95p and RX5day (Fig. 5(b)). More than half of RCMs show increasing trends for these indices, though they are not statistically significant. RX1day has increasing (not significant) observed trend and most of RCMs model before and after bias correction also have increasing trend, though not significant. More than half of RCMs show increasing trend both before and after bias correction for R20 (not significant) but observations show significant increasing trend. In case of cwd, about half of the model show decreasing trends (not significant) while it is observed to be decreasing significantly.

In summary, for temperature indices like TX90p and TN90p, modelled trends in climate extremes agree with the observed trends for many RCMs with significant results while for indices like TNn and TXn, they do not agree (not significant). For precipitation indices, more than half of RCMs agree with observations but the results are not statistically significant as compared to observations. And, bias correction has no significant influence in either increasing or decreasing trends except for few cases.

4.2. Precipitation extremes

4.2.1. Historical and projected future trends in precipitation extremes

Trends in precipitation extreme indices during the historical period of 1980–2005 and future periods at eight stations in the EER watershed are presented in Fig. 6. The statistical significance of the trends was tested using Modified Mann-Kendall test and Spearman's rho test. The colours in Fig. 6 show magnitude of Sen's slope of the trend line. Observed trends are shown in circle, and '+' sign is provided inside circle for significant trend conducted at $\alpha = 0.05$ (Spearman's rho test). For each of the observed indices, number of stations that have significant trends vary from one to a maximum of five among the eight stations. For instance, observed RX1day trends are significant for three stations, namely, 903, 904 and 919. Heavy rainfall amounts like maximum 1-day precipitation (RX1day), maximum consecutive 5-day precipitation (RX5day) and very wet day precipitation (R95p) are observed with increasing trends. RX1day precipitation is increasing at a rate of 0.5 to 9 mm/year (approx.) while RX5day precipitation is also increasing at a rate to 2 to 17 mm/year. Similarly, R95p is also on rise by 6 to 50 mm/year. This result aligns with the increasing trends of extremes in Nepal as discussed in Baidya et al. (2008) and Karki et al. (2017). However, Karki et al. (2017) claims the decreasing precipitation extremes in the central lowlands. This contrasting results may be due to – (a) exclusion of the stations in the ERR in Karki et al. (2017) and (b) difference in the scale of the study: this study is focused on small scale catchment unlike the study by Karki et al. (2017) which focused on entire Nepal. In the ERR basin, consecutive dry days (CDD) are increasing with simultaneous decrease in consecutive wet days (CWD). But at most of the stations, trends are statistically insignificant. Similarly, the numbers of heavy rainfall days are also increasing by 0.25 to 1.7 days/year as suggested by increase in R20 index, and four stations show statistically significant increasing trends. Total wet days precipitation amount (PRECTOT) in the ERR watershed is also increasing by about 8 to 105 mm/year and the trends at five among the eight stations are statistically significant. Hence, historical trends from 1980 to 2005 clearly show that precipitation extremes are increasing every year in the ERR watershed.

Trends in the projected precipitation indices in near future, middle future and far future periods, on the other hand, have mixed trends unlike observed trends as shown in Fig. 6. Only few RCMs shows significant trends for future projections– the numbers of which are shown inside the grid box, and magnitude of slope are less than observed trend.

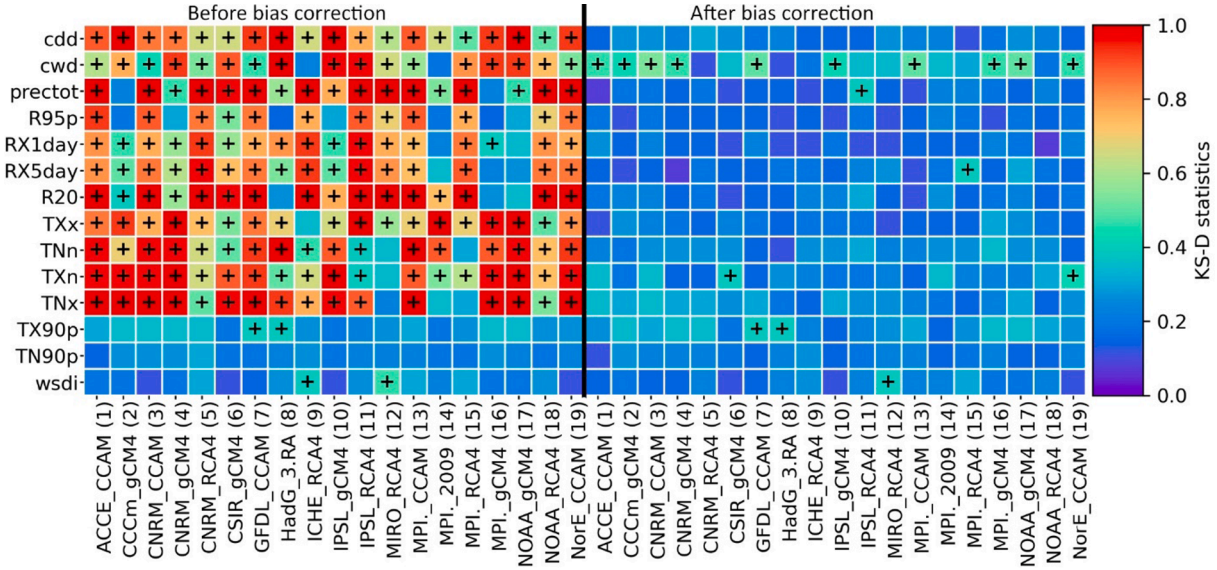

Fig. 5a. Differences in distribution of extreme indices between observation and RCM for historical period 1980–2005 shown using Kolmogorov-Smirnov D statistics ('+' sign indicates significant result at $\alpha = 0.05$).

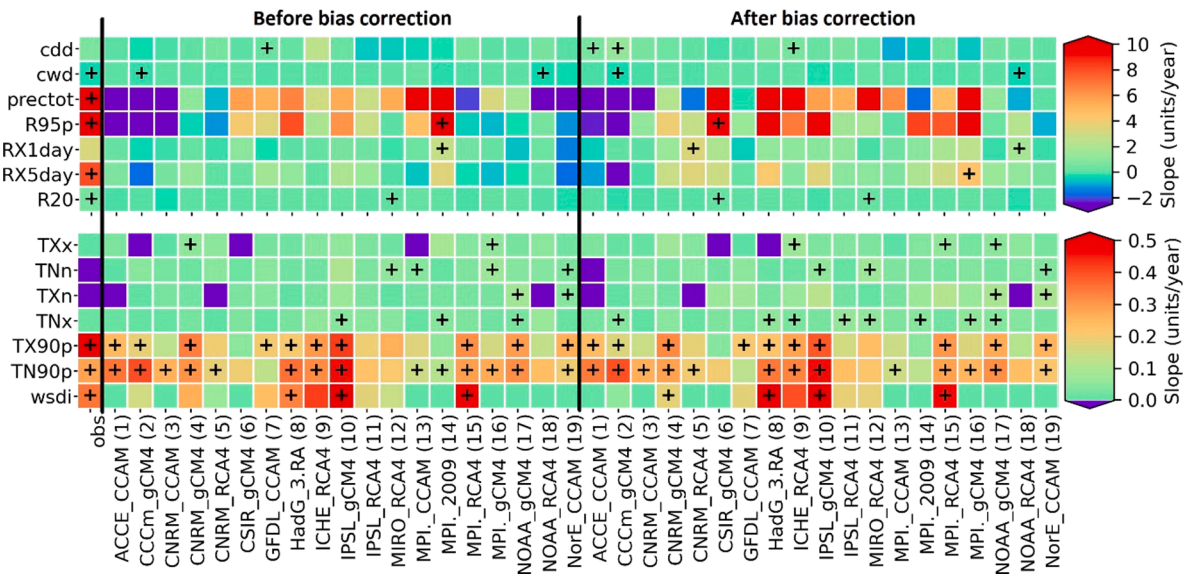

Fig. 5b. Variation in trends of extreme indices in observation and RCMs for historical period 1980–2005. Sen's slope are provided. 'units' represent corresponding units of extreme indices. '+' sign indicates significant trend at $\alpha = 0.05$ with Modified Modified Mann-Kendall test.

Projected CDD trends from RCMs in future are negative for most of the stations and they range from −0.7 to 0.5 days/year in contrast to positive historical trend of greater than 0.7 to 1.4 days/year. On the other hand, decreasing CWD trends are projected which is consistent with observed trend. Projected PRECTOT trends vary among stations differently in different future periods, most of them increasing, even though historical trends are significantly positive for majority of the stations. Though the future PRECTOT trends varied from decreasing 3 mm/year to increasing 15 mm/year, they are less in compare to magnitude of observed trend. Positive projected R95p, RX1day and RX5day trends are observed for most of the future periods with up to 10 mm/year, 1.5 mm/year and 3.5 mm/year respectively. Projected R20 trend varies between decreasing 0.1 days / year to increasing 0.3 days / year and most of the stations show increasing trends like the observed trend, though observed trend is higher in magnitude.

Alongside with the trends, indices as PRECTOT, R95p, RX1day and RX5day are projected to increase in futures as discussed in section 4.2.3. Any local small scale extreme inducing processes, like in the study, are tied to larger scale phenomenon, here in this case, to the overall monsoon in Nepal. Precipitation regime in the Himalayan region in Nepal is largely determined by Indian Summer Monsoon (ISM) and precipitation extremes like RX1day, RX5day, CWD, R95p and R20 occur usually during monsoon season for June to September. In addition, the South Asia's Himalayas, a regional topographic feature, also modulates the distribution of extreme precipitation events (Singh et al., 2019). Singh et al. (2019) discusses about the increase in intensified sub-seasonal extremes across parts of India and an increase in spatial variability of rainfall despite an overall weakening of seasonal rainfall in the monsoon core. They attributed this overall weakening behaviour of monsoon, but intensified local events, to global warming and anthropogenic factors, mainly, the influence of aerosols, land-cover changes and agricultural intensification. Any intensification of ISM in future in the Himalayan region, as discussed in Sanjay et al. (2017), might play a key role in increasing trends and magnitude of extreme indices. Suman and Maity (2020) showed that areas adjoining north India (including the Himalayas and Tibetan Plateau) are projected to experience significantly higher mean daily air temperature at 850mb in future scenarios thereby providing conducive environment for an increase in water holding capacity of the atmosphere according to Clausius-Clapeyron relationship. This will also enhance physical processes for increase in extreme precipitation events. They argued that relative higher increase in precipitable water content in comparison to the Tibetan plateau region creates favourable condition for enhancement of ISM that in turn increase the extreme rainfall events. Enhancement of the thermodynamics conditions due to atmospheric warming cause the increase in ISM as well its daily variability that are linked to increase in heavy precipitation and decrease in both low rain-rate and number of wet days during future monsoon (Sharmila et al., 2015).

4.2.2. *Spatial variation of trends in precipitation extreme indices*

Fig. 6 illustrates spatial variation in the extreme precipitation indices across eight stations in the ERR watershed. Increasing and decreasing trends along with the magnitude of slope of linear trend line are shown by positive and negative values of Sen's slope with colours. Likewise, statistical significant trends as tested by Spearman's rho test at 95% level of confidence are shown by '+' inside observation circles. The division of the physiography of the study area is marked by Hills and Tarai/Siwalik as backdrop in Fig. 6. Hills stations (904 and 905) have elevations above 1,500 m above the mean sea level (masl) while rest of the stations have elevation ranging between 250 and 1050 masl. As stated above, most of the extreme indices have increasing trend in the study area except consecutive wet days (cwd). However, it is interesting to note that magnitude of trend at the highest elevation, station 905 at elevation around 2,314 m, is lower than the stations located at lower elevations. Though its neighbouring stations 904 (at elevation around 1706 m), 906 (at elevation 474 m) and 919 (at elevation 1030 m) show higher amount of trends in the extreme indices. This can be due topographic effects in the regions. Other stations with elevations less than 350 m are located at plains and show similar magnitudes of trends. Trends of the indices representing heavy rainfall magnitude and frequency are increasing at faster rate in station 919 (Makawanpur Gadhi) than the surrounding stations with statistically significant results. Magnitude of trends of extreme indices is less at the highest elevation station than other stations, however, there is not enough evidence that Hill stations and Tarai/Siwalik stations behave differently in terms of trends in extreme indices.

Compared to observed spatial trends, future trends have less spatial variation among the stations and less magnitude of slope. They are shown in Fig. 6. This can be attributed to limitations of RCMs being unable to capture spatial heterogeneity as they have coarser resolution.

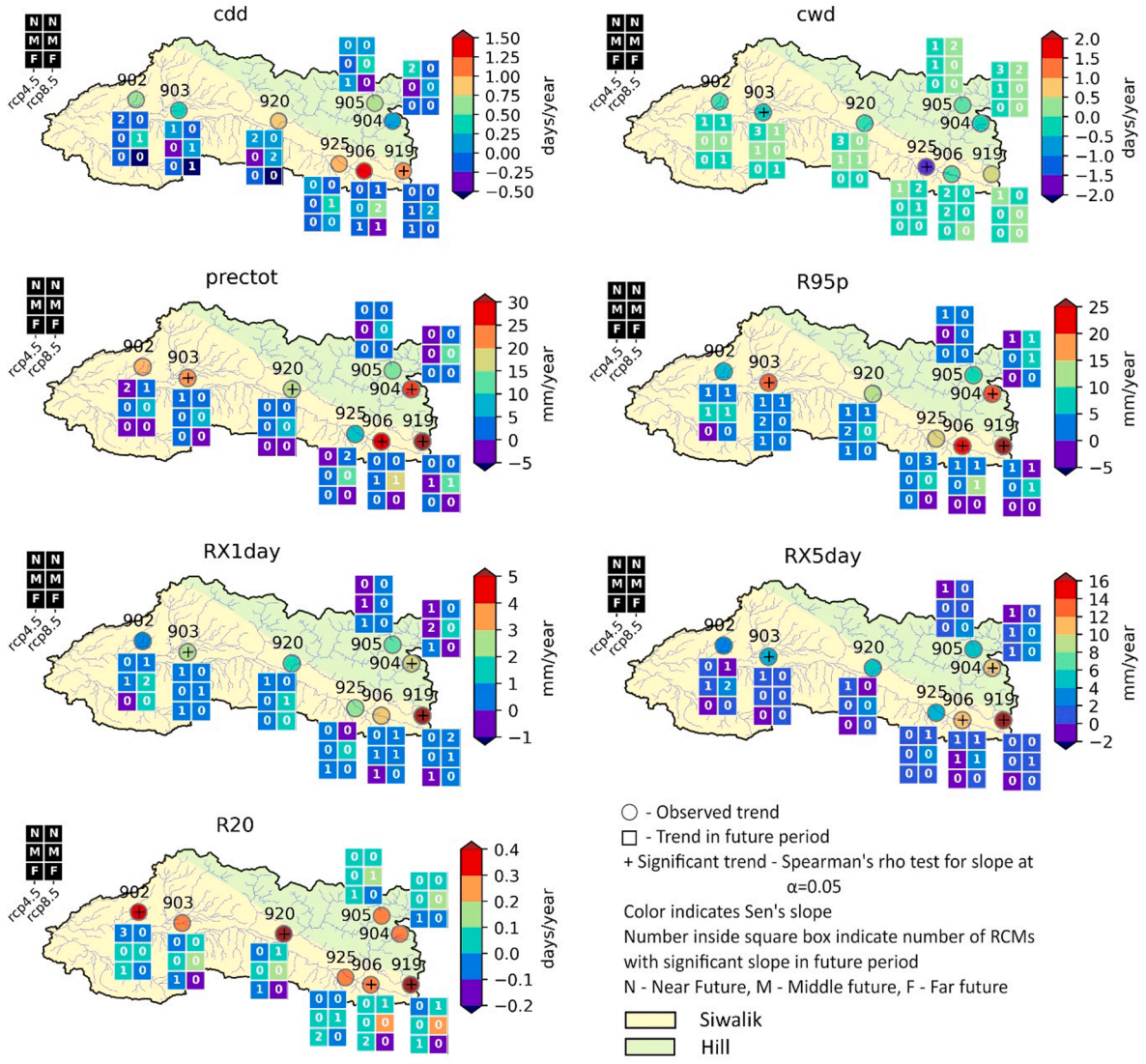

Fig. 6. Spatial variation of trends in precipitation-related extreme indices for the historical (1980–2005) and future periods.

4.2.3. Projected changes in future precipitation extremes

Projected changes in the seven precipitation extreme indices at eight stations in the ERR watershed for different future periods under RCP 4.5 and RCP 8.5 scenarios are shown in Fig. 7. These changes are multi-model ensemble means of different RCMs. Only few RCM models show statistically significant projected changes (tested using two sample T-test at $\alpha = 0.05$) as shown in Fig. 8. CDD at most of the stations in the ERR watershed are projected to increase within the limits of 12% in future. For RCP 4.5, increase in CDD, averaged over all stations, are between 0.7 and 1.6% from the historical average of 68 days while projected changes in RCP 8.5 varies from 2 to 6%; the highest change occurring at FF. In complement to CDD, CWD at majority of those stations are projected to decrease by less than 20%. For RCP 8.5 scenario, in FF, many stations show decrease by >15% in CWD. In general, CWD is projected to decrease between 2 and 7%, except being FF, from the historical average of 22 days. Shrestha et al. (2017) also found increase in rainfall intensities with decrease in CDD thus indicating the rise of extreme events in the eastern Nepal in historical period. PRCPTOT is projected to increase for all future periods for both the scenarios. In RCP 4.5 scenario, PRCPTOT is expected to increase within 3% in NF and within 8% in MF and FF on the historical mean of 2106 mm. For RCP 8.5 scenario, it is projected to increase between 6% and 10%, though some of stations show increase above 15%. For heavy rainfall indices like R95p, RX1day and RX5day, projected changes increase as we go more into future; and they show more changes in comparison to other indices. R95p is also projected to increase in considerable amount. In NF, under RCP 4.5 scenario, basin averaged R95p is projected to increase by 13% and this is expected to increase up to 30% in MF FF against the historical mean of 557 mm. Under RCP 8.5 scenario, stations in the ERR watershed are expected to receive increased R95p by 20% to 60% in future. Results are also similar in case of RX1day and RX5day precipitation extreme indices. RX1day is projected to increase by 10 to 25% and by 20 to 35% in the ERR watershed for RCP 4.5 and RCP 8.5 scenarios respectively. Similarly, amount of changes in percentage are expected for RX5day too. These results are consistent with study by Baidya et al. (2008), which showed increase in extreme precipitation indices (RX1 day, RX5day, heavy precipitation days, total precipitation) in more than half of 26 stations encompassing majority of climatic zones of Nepal in the historical base period. Heavy rainfall days (R20), on an average for all stations, are also expected to increase between 1 and 4% except in FF in RCP 8.5 scenario which project a decrease by about 0.6% from its historical average of 34 days.

Increasing future trends and projected changes in extreme-indices related to precipitation in the EER watershed expected in future. Increase in precipitation amount, dry days and heavy precipitation events are projected in future. Since, indices like R95p, RX1day and RX5day are

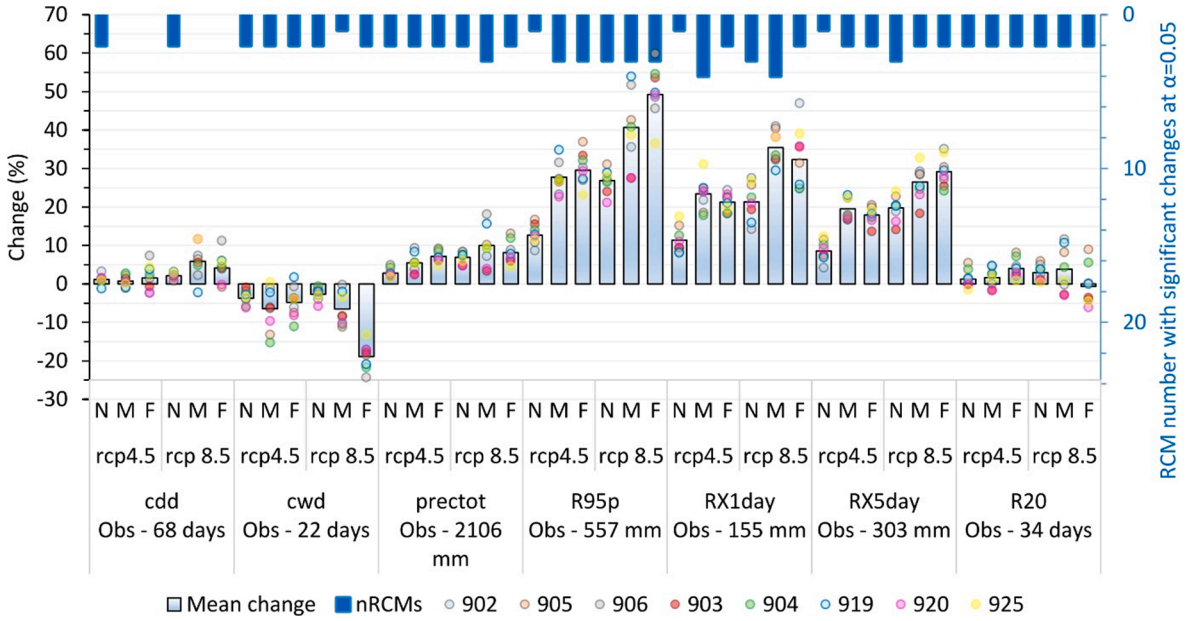

Fig. 7. Projected changes in future precipitation extreme indices compared to historical (1980–2005) *Notes: Changes in the indices are expressed in percentage from the baseline period of 1980–2005. N, M and F represent near future (2021–2045), mid future (2046–2070) and far future (2071–2095) periods.*

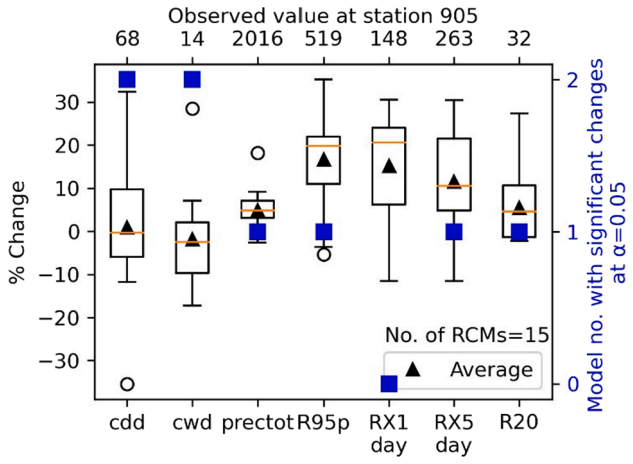

Fig. 8. Uncertainty in RCM models- Projected changes by 15 RCMs in consensus in near future for RCP 4.5 scenario for station 905. *Notes: Box plot extends from the lower to upper quartile values of the data, with a line (red) at the median. The whiskers are positioned at 1.5 times of Inter-Quartile Range from the quartiles. Black triangles are multi model mean values, while blue squares are number of RCM models that show significant projected changes in future, tested at α = 0.05 using Two-sample T-test.*

closely associated with hydrological extremes as floods and events like landslides, those events are also expected to increase together with precipitation extreme events.

Fig. 8 provides an illustration of the uncertainties associated within the models. As an example, a box plot of changes in precipitation extreme indices in NF compared to 1980–2005 at station 905 is shown. Range of projections by RCMs (N = 15) are quite wide spread. For instance, RX1day ranges from approximately 10% decrease to about 30% increase with an average of about 15% increase. Besides, the RCMs that projected significant changes (T – test at α = 0.05) are quite less – maximum of 2 RCMs. It is clear, from Fig. 8, that the spread of future changes among ensemble members is large even taken within the consensus case.

4.3. Temperature extremes

4.3.1. Historical and projected trends in temperature extreme indices

Temperature-related extreme indices at the three stations in the EER watershed during historical period show mixed trends (Table 4 and Fig. 9). Maximum of daily maximum temperature (TXx) shows increasing trends at two stations (905 and 906) at a rate of 0.04 °C/year, but tests for Sen's slope (Spearman's rho test) show insignificant results. Likewise, trends in maximum of daily minimum temperature (TNx) are decreasing at the rates of 0.055 – 0.067 °C/year at stations 902 and 906, however, station 905 shows increasing trend at rate of 1.25 °C/year. In case of minimum of daily maximum temperature (TXn), two stations 902 and 905 show decreasing trend at the rates of 0.186 and 0.05 °C/year, respectively, while station 906 show increasing trend. The results are statistically significant only at the station 902. For minimum of daily minimum temperate (TNn), stations 902 and 906 show increasing and decreasing trends, respectively, and station 905 show no change. None of them are statistically significant. However, all the stations show increase in warm days (TX90p) by 0.2–0.7% per year and results are statistically significant for two stations. Likewise, stations 902 and 905 also show increase in warm nights (TN90p) by 0.3–0.5% per year and both of results are significant. Increase in warm days and warm nights in ERR is consistent with the findings of Baidya et al. (2008) and Shrestha et al. (2017). However, station 906 show decreasing trend by about 0.1% (statistically insignificant). Finally, for all the stations, there is no change in warm spell duration index. Historical period (1980–2005), therefore, clearly shows increase in warm nights and warm days, and no change in warm spell duration; however, for other indices we observed mixed results.

Unlike mixed observed trends at three stations, projected temperature indices have consistent increasing trends in future (exception being TNx, TNn and TX90p for RCP 4.5 in FF), as shown in Fig. 9. TXx has increasing trend from 0.02 to 0.06 °C per year in NF while from 0 to 0.04 °C per year in MF and FF. TNx, TXn and TNn are also projected to increase by 0.01 to 0.1 °C per year in future. Warm days and warm nights also have increasing trends at rate of 0–1.2% of days/year in future and so as warm spells (upto maximum of 2.5 days/year. Relatively higher number of RCM models with statistically significant results for temperature based indices show that results are consistent among RCM models.

Table 4
Historical (1980–2005) trends in temperature extreme indices in the EER watershed.

Indices	Stations	Mann-Kendall's Tau	p- value from M−MK test	Sen's slope		p –value from Spearman rho test	Significance (α = 0.05) as per M−MK test	Significance (α = 0.05) as per Spearman's rho test
TXx	902	−0.157	0.181	−0.044	↓	0.221	NS	NS
	905	0.145	0.233	0.04	↑	0.238	NS	NS
	906	0.142	0.320	0.04	↑	0.217	NS	NS
TNx	902	−0.345	0.013	−0.055	↓	0.012	S	S
	905	0.474	0.001	0.125	↑	0.001	S	S
	906	−0.218	0.122	−0.067	↓	0.122	NS	NS
TXn	902	−0.428	0.002	−0.186	↓	0.006	S	S
	905	−0.163	0.251	−0.05	↓	0.291	NS	NS
	906	0.111	0.439	0.053	↑	0.425	NS	NS
TNn	902	0.194	0.000	0.045	↑	0.167	S	NS
	905	−0.012	0.947	0	↕	0.973	NS	NS
	906	−0.043	0.774	−0.008	↓	0.853	NS	NS
TX90p	902	0.268	0.058	0.235	↑	0.068	NS	NS
	905	0.569	0.002	0.492	↑	0	S	S
	906	0.526	0.009	0.678	↑	0	S	S
TN90p	902	0.514	0.000	0.332	↑	0	S	S
	905	0.443	0.002	0.488	↑	0.001	S	S
	906	−0.089	0.537	−0.118	↓	0.609	NS	NS
WSDI	902	−0.012	0.944	0	↕	0.874	NS	NS
	905	0.255	0.080	0	↕	0.034	NS	S

Notes: Arrows ↑, ↓ and ↕ indicate increase, decrease and no change in trends respectively. 'S' and 'NS' are statistically significant & not significant.

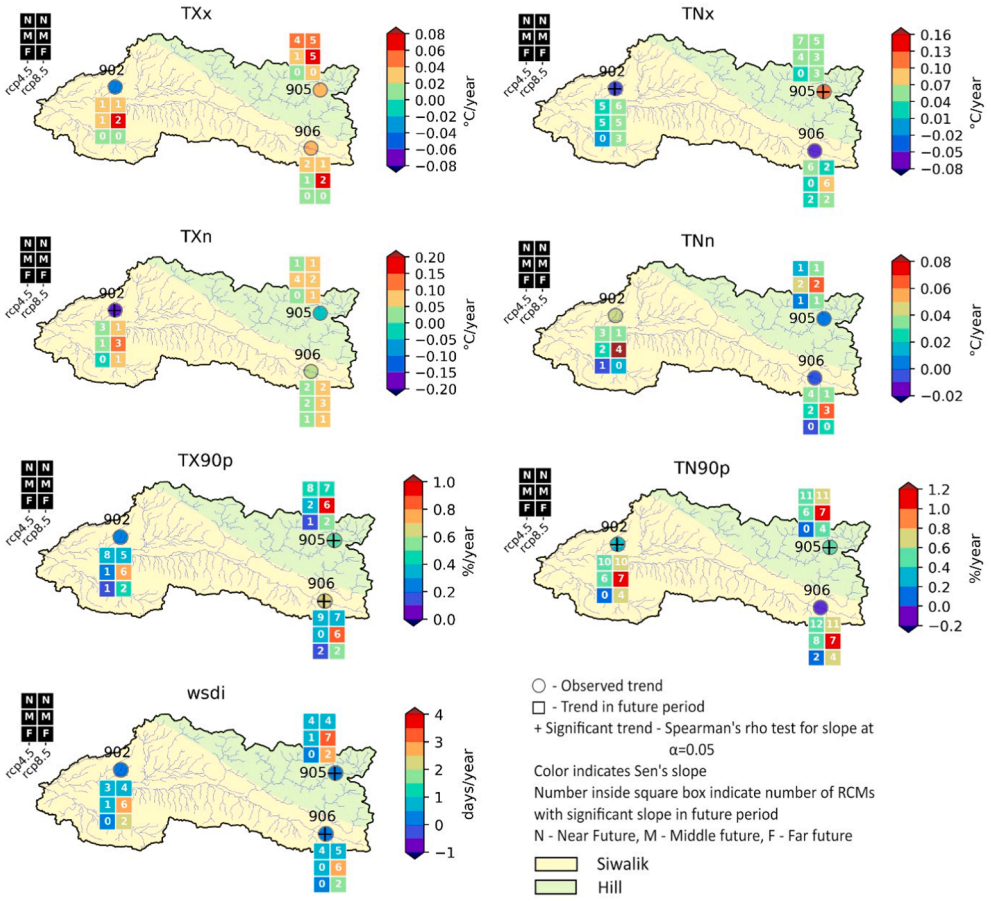

Fig. 9. Spatial variation of trends in temperature-related extreme indices for the historical period (1980–2005).

4.3.2. Spatial variation of trends in temperature extreme indices

Table 4 provides information on spatial variation of temperature-related ETCCDI extreme indices for the historical period in the ERR watershed. Only three stations had the temperature recorded, namely, stations 902, 906, and 905, at the elevations of 256 m, 474 m, and 2,314 m, respectively. There is not enough evidence (as there are only three stations) to deduce a clear relationship between the dependency of extreme indices with elevation or with physiographical region in this watershed. However, there is an overall increase in the warm days and warm nights in the region and no change in the warm spell duration index. Fig. 9 also shows spatial variations in indices among three stations. Future trends are similar in terms of magnitude and direction

though for TXx and TX90p, trends in NF at station 905 is stronger than at remaining stations. Like precipitation based indices, these trends are similar spatially.

4.3.3. Projected changes in future temperature extremes

Three future periods (NF, MF and FF) are considered for analysing future trends under two scenarios, namely, RCP 4.5 and RCP 8.5. The projected changes in future trends with respect to baseline are illustrated in Fig. 10. All the temperature-related extreme indices, in general, are projected to increase in future periods, in which increase is more pronounced under the RCP 8.5 scenario. Majority of ensemble RCM members show significant changes (tested using two-sample T- test at $\alpha = 0.05$) in future from historical values for temperature based extreme indices, which is in contrast with extreme indices for precipitation. Maximum of daily maximum temperature (TXx) are projected to increase by around 1 °C to 1.7 °C in NF, 1.2 °C to 3.1 °C in MF, and 1.3 °C to 4.1 °C in FF. Likewise, maximum of daily minimum temperature (TNx) are also projected to increase by around 1.5 °C to 2.5 °C in NF in both scenarios. Increase in TNx are much higher ranging from 2 °C to 5 °C in MF and FF, which suggests that increase in TNx is likely to be more than TXx in future. Minimum of daily maximum temperature (TXn) are also projected to increase by 0.2 °C to 1.3 °C in NF for both scenarios, though the rise of TXn in MF and FF is by 1 °C to 5 °C in MF and FF. Magnitude of increases are slightly lower for minimum of daily minimum temperature (TNn) than TXn. Furthermore, warm days (TX90p) are projected to increase from about 10% up to 15% in NF. They are expected to increase by 16 to 20% in MF and FF in RCP 4.5 scenario, while expected increase is by 30% to 50% in RCP 8.5 scenario for those futures. Similarly, warm nights (TN90p) will increase by 15% to 20% in NF in both scenarios. They are expected to increase between 25% and 30% in MF and FF in RCP 4.5 scenario, while expected increase is by 45% to 60% in RCP 8.5 scenario for those futures. In is clear from above data, that nights are going to be much warmer in future. In addition, warm spell duration index (WSDI) is projected to increase by between 20 and 30 days in both scenarios in near future. Projected increase in MF and FF in RCP 4.5 scenario is between 35 and 40 days, though it is very high (from 80 to 120 days) in RCP 8.5 scenario. These results clearly indicate potential rise in temperature-related extreme events in the EER watershed. Hotter days and nights are expected to increase in future together with the rise in extremes, and further coupled with other precipitation related extremes, may result in compounded impacts on societies and ecosystems in future. Projected changes for the station 905 (hill station) is higher than other two stations.

Fig. 11 provides an example of the uncertainties associated within the RCM models. It is a box plot of changes in temperature based extreme indices in Near Future compared to 1980–2005 for station 905. Here, number of RCMs in an ensemble of consensus case is 15. Spread of projected changes are large, for instance, for station 905, warm spell duration index (wsdi) ranges from approximately increase in 3 days to about 49 days with an average of about 24 days. It is clear from Fig. 11 that uncertainties among the models are present and they are large even though attempts were made to address it using consensus case.

4.4. Hydrologic alterations and extremes

Hydrologic alterations in three stations in the EER watershed, namely, Q460, Q465 and Q470 are illustrated in Fig. 12(a), Fig. 12(b), and Fig. 12(c) respectively. Discussions are made in following sections.

4.4.1. Hydrologic alterations in monthly streamflow

Fig. 12 illustrates hydrologic alteration (HA) factors for monthly streamflow magnitudes (parameter group 1) at three stations, and Fig. 13 presents monthly flow changes (in median) from pre-1990 period to post-1990 period. Hydrologic alterations in monthly streamflow, it is interesting that middle RVA categories at stations Q460 and Q465 for 11 months and at station Q470 for seven months show negative alterations, most of which are middle and high degree of alterations. This means that the frequency of values in middle category has decreased from pre-1990 period to post-1990 period. In station Q460, median values in dry months like Jan, Feb and March has increased by 20–35 percent in post-1990 period but has decreased in monsoon months of Jun, Aug and Sep by about 20–30 percent (Fig. 13). HA factors relating monthly flows in high and low RVA categories for stations Q460 and Q465 are positive for most of months with middle and high degrees (hydrologic alteration values >0.5 or 50%). For station Q465, HA factors for low RVA category also shows decline like middle category, but with increase in high category for all months. It is to be noted that, for station Q465 even though HA factors are negative, there is increase in median values for all months ranging from 15% in December to 170% in June, except in September (Fig. 13).

Deviations in median values for monthly flows at station Q470 are less in comparison to other two stations. Shifts in HA factors relating to group 1 (or monthly flows) from middle range category to high and low RVA categories before and after 1990 is an indication of shifts in the frequency of monthly flows towards higher and lower percentile groups. This implies increase in the intra-annual hydrological variability in the river flow. Such changes are not visible in annual volume point-change analysis as carried out by Pandey et al. (2020), though they can be

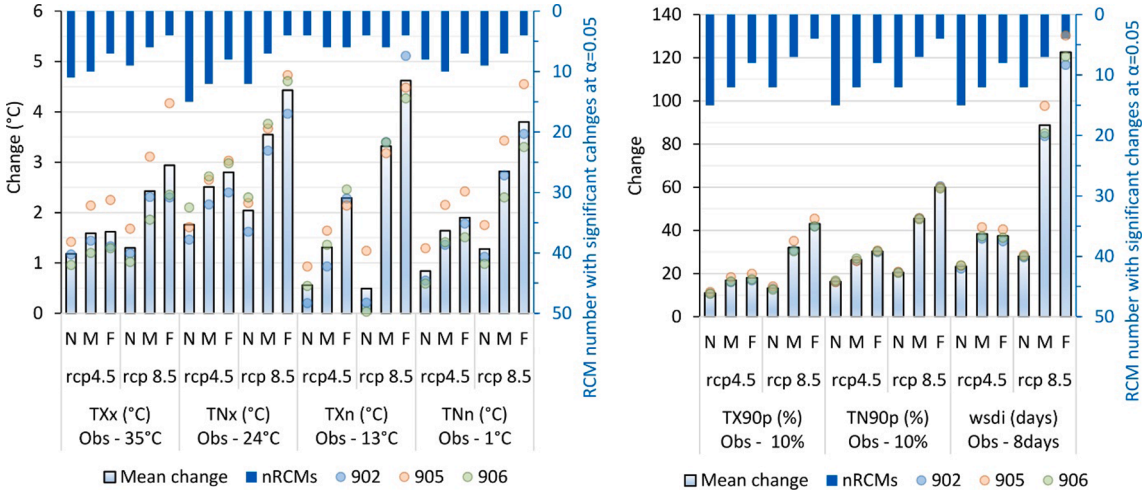

Fig. 10. Projected change in future temperature based extreme indices compared to historical baseline (1980–2005) - (left) for indices TXx, TNx, TXn and TNn; (right) for indices TX90p, TN90p and WSDI. N, M and F represent near future (2021–2045), mid future (2046–2070) and far future (2071–2095) periods.

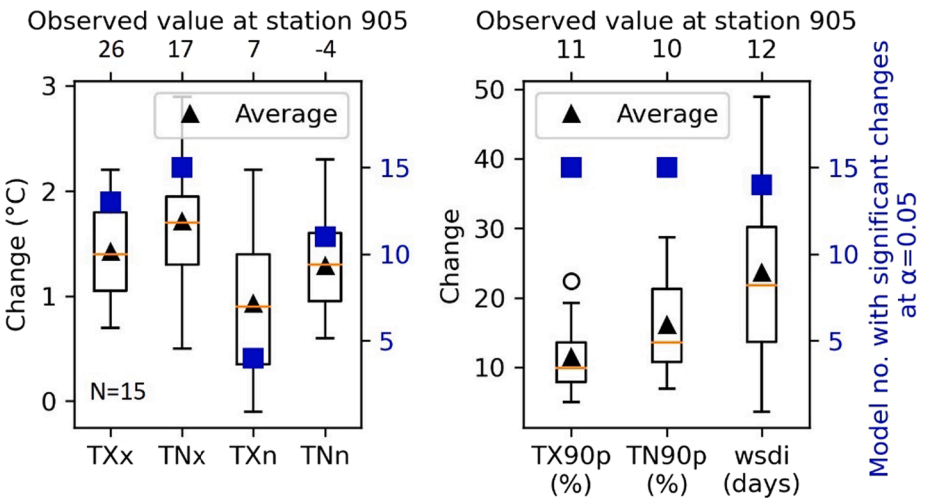

Fig. 11. Uncertainty in RCM models- Projected changes by 15 RCMs in consensus in near future for RCP 4.5 scenario for station 905 (left for indices TXx, TNx,TXn and TNn; right for indices TX90p, TN90p and wsdi). Other descriptions are same as in Fig. 8.

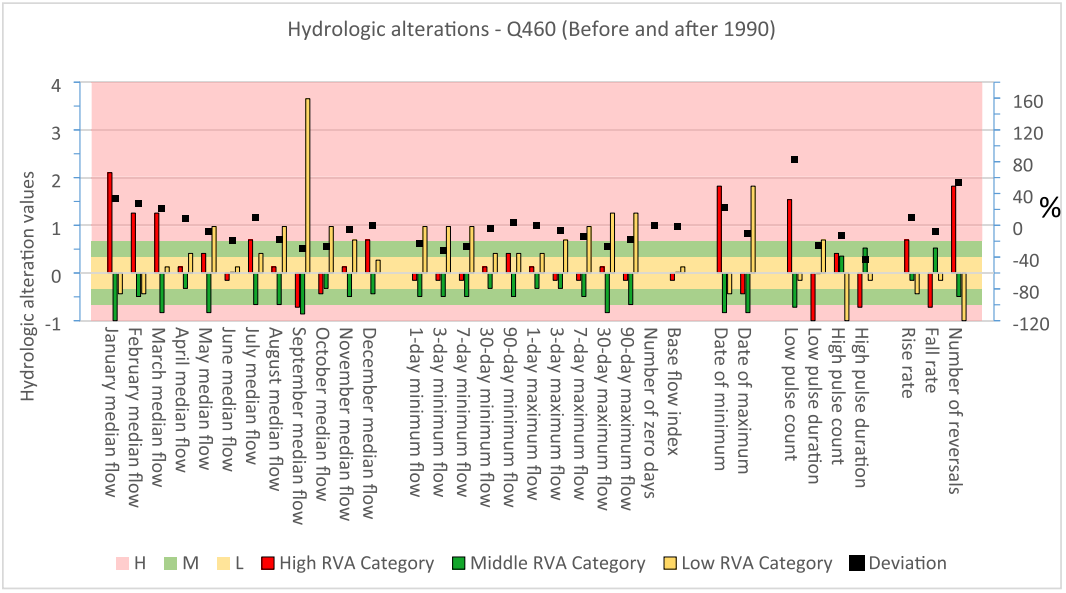

Fig. 12a. Hydrologic alteration in station Q460 before and after 1990 for three RVA categories.

attributed to anthropogenic changes after 1990. It is to be noted that, there is no change in the seasonal pattern of precipitation before and after 1990 (Fig. 13d).

4.4.2. Alterations in annual extreme flow conditions

Low flows: Parameter group 2 represents extreme flow conditions. Hydrological alterations in these flow conditions before and after 1990 are also presented in Fig. 12. Almost all of minimum and maximum flows parameters for middle RVA category at three stations have negative HA values and most of alterations are of medium and high degree. In case of minimum flow parameters (1-day, 3-day, 7-day, 30-day and 90-day minimum flows), station Q460 show negative HA values for high RVA category, result of which is shown by increase in low RVA category. For station Q465, high RVA category show high positive alterations. Alteration of low flows is of low degree for station Q470. Low flow magnitudes at station Q460 varies from about 4% increase for 90-day minimum flow to about 32% decrease for 3-day minimum flow in post-1990, among which only 90-day minimum flow has increased. At station Q470, minimum flow has decreased from 2 to 16 percent. Trend analysis of 1-day, 7-day and 30-day minimum flow for period 1980–2005 are presented in Table 5. They represent short-term, medium term and long-term minimum flow regimes. At station Q460, 1-day and 7-day minimum flow are observed to be decreasing at 0.066 m^3/sec per year; while 30-day flow is increasing at 0.011 m^3/sec per year. At station Q465, minimum flows are increasing at rate of 0.018 to 0.034 m^3/sec per year. In contrast, minimum flows are decreasing by about 0.004 to 0.015 m^3/sec annual. However, all these trends are not statistically significant.

The possible impact of decrease in low flows can be reduction of habitat availability (Zeiringer et al., 2018). Importantly, since these rivers have low flows in winter (DJF) months than in monsoon (JJAS), reduction in water flow can have serious implication on environment and aquatic habitat. For instance, Abebe et al. (2020) reported that extreme reduction in low flows in Gumara River in the Ethopian highlands impacted on predators by reducing their mobility and ability to access prey concentrated in smaller pools. Unlike these two stations, minimum flows have increased at station Q465; 1-day minimum increased by about 15% and 30-day minimum by about 35% after 1990.

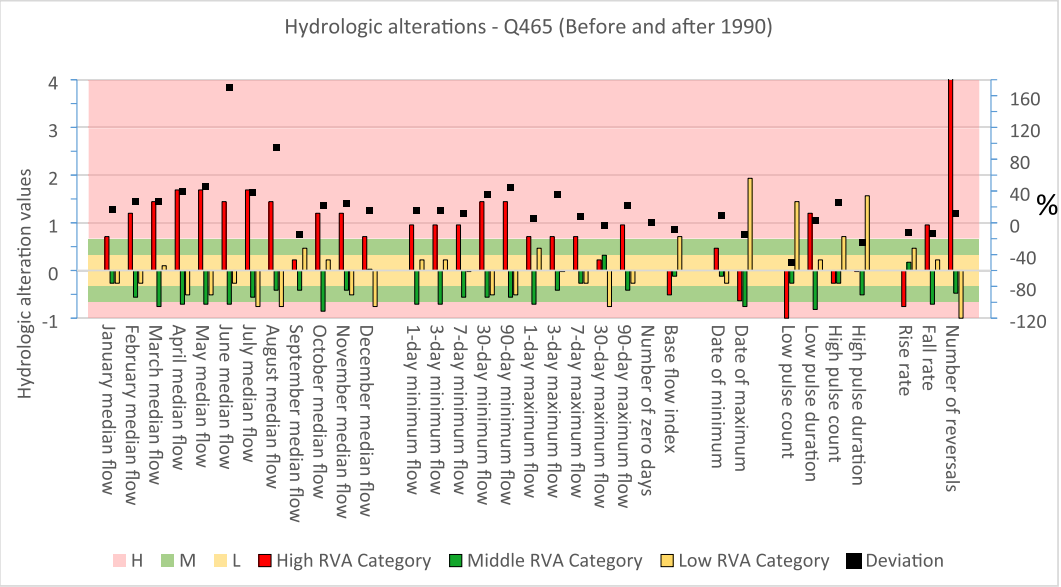

Fig. 12b. Hydrologic alteration in station Q465 before and after 1990 for three RVA categories.

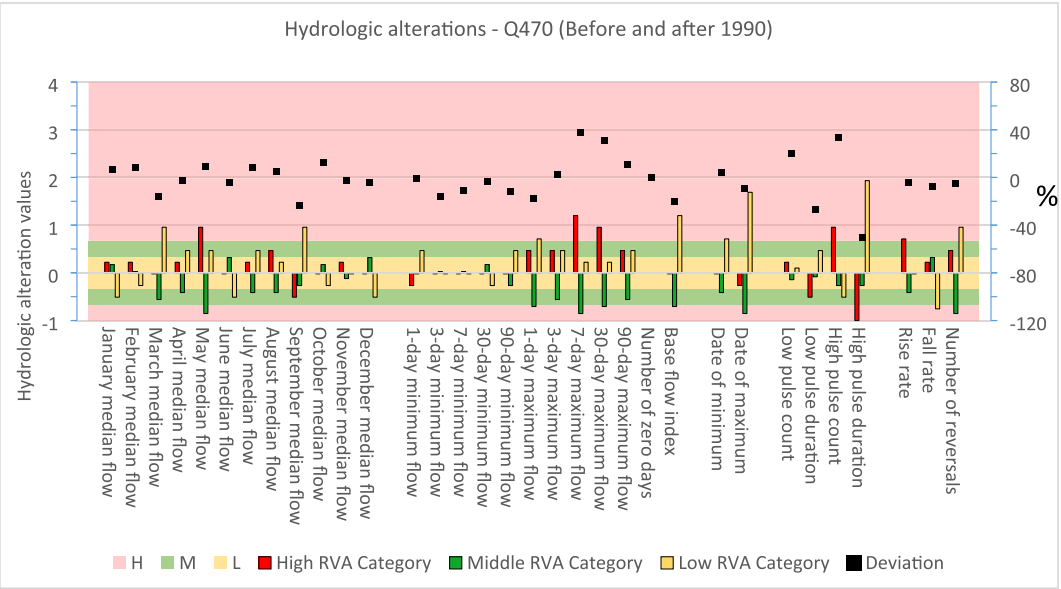

Fig. 12c. Hydrologic alteration in station Q470 before and after 1990 for three RVA categories *(Notes: H, M and L represents high, medium and low degree of alterations, respectively. Hydrologic alteration values within yellow, green and light-red zones represent low (0 to 33%), medium (34 to 67%) and high (>67%) degree of alterations, respectively. Deviation values are computed from the median values before and after 1990, and expressed as percentage in secondary axis which are shown as squared dots.)*

High flows: Pattern of high flow HA values for station Q460 is similar to that of low lows i.e. negative high and middle RVA categories are observed when low RVA category is positive. At this station, high flows in post 1990 has decreased in general; for instance, seasonal maximum flow (90-maximum) has decreased up to 19 percent and weekly maximum (7-day) has decreased by about 15 percent. This contrasts with station Q465 and Q470, where there is increase of high flow regimes up to 37 percent. In station Q465, seasonal maximum flow (90-maximum) has increased up to 27 percent and weekly maximum (7-day) has increased by about 8 percent. Most of alterations for Q465 are positive for high RVA category and negative for medium and low RVA category. Likewise, in station Q470, seasonal maximum flow has increased by 11 percent and weekly maximum by about 37 percent; though 1-day maximum has decreased by 18 percent. At station Q470, HA values are positive in high and low RVA categories but negative in middle category. Results of trend analysis of high flows namely, 1-day maximum, 7-day maximum and 30-day maximum flows for period 1980–2005 show that they are increasing annually in the EER watershed (Table 5). 1-day flow is increasing at rate of 2.3, 9.1 and 1 m^3/sec per year at stations Q460, Q465 and Q470 respectively. 7-day and 30-day maximum flows are also increasing at rate between 1.2 to 4.5 m^3/sec and 0.4 to 1.8 m^3/sec annually respectively. Though these trends are not statistically significant, they provide information on increasing short, medium and long term flow regimes.

Increase in the high flow regimes can have both positive and negative impacts which depends up on channel morphology, types of substrate, depth and other geomorphological characteristics and greater magnitude of extreme flows can also disrupt life cycle, loss sensitive species (Zeiringer et al., 2018); but reductions of seasonal maxima also can break the linkage between flood-plains and surrounding

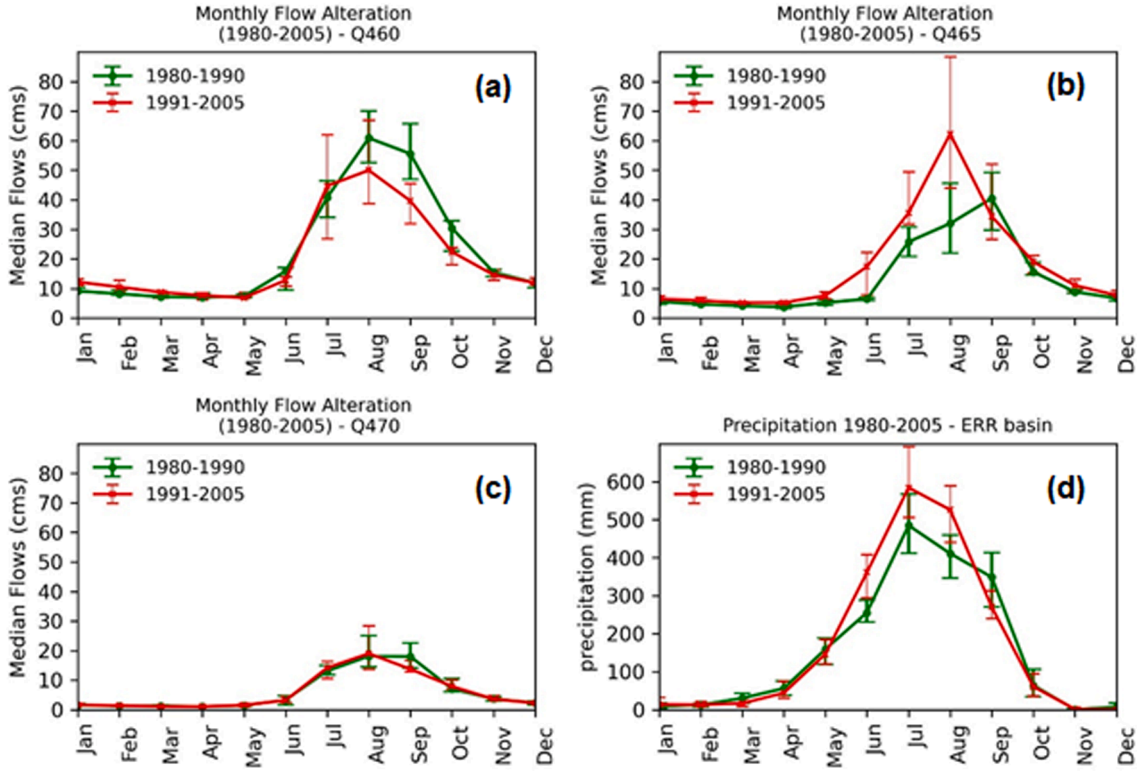

Fig. 13. Alterations in monthly flow and precipitation in the Extended East Rapti (EER) watershed before and after 1990. Spread represents Middle RVA category (34th to 67th percentile). cms is cubic meters per second.

environmental habitats (Abebe et al. 2020). We recommend for detailed study on impacts of flow regimes on corresponding ecological responses.

Base flow: Number of 'zero-day' values for all stations is zero, and there in no alteration in this parameter before and after 1990. Changes in base flow index HA values is low alteration for station Q460. At station Q465, there is medium alteration (negative) of high RVA category with simultaneous high alteration (positive) of low RVA category. This is shift in frequencies from high to low category. In contrast, at station Q470, there is high alteration (negative) of middle RVA category when low RVA category show positive high alteration. This implies shift in frequencies from middle to low categories. Likewise, median value has decreased by about 20 percent at station Q470 while there are only small changes in remaining stations.

4.4.3. *Timing of daily minimum and maximum flows*

Table 6 presents shifts in occurrence dates of 1-day maxima and minima in three rivers in the study area (Parameter group 3). Median Julian date of annual 1-day minimum flow for all three rivers are moving backward in time, which suggests prolongation of low flow season. Similarly, median Julian date of annual 1-day maximum flow for all three rivers are occurring almost a month earlier. Such changes can also be observed from the trends of the date of minimum flow (days) and maximum flow in Table 6. Date of maximum flows is in decreasing trend, i.e., it is occurring earlier by 1 day to 2 days per year in period of 1980–2005; however, this decrease is statistically significant only for station Q465. Similarly, date of minimum flows is shifting later for stations Q460 and Q465 by around 1 to 1.5 days; but is shifting earlier in station Q470. Trends for date of minimum flows though are not statistically significant.

Such shifts in low and high peak flows indicates the changing flow regimes and increase in variability of river flow in the EER watershed, either due to natural or anthropogenic causes. Such alterations can have serious implications on natural habitats and ecology of a river which needs detailed investigation.

4.4.4. *Alterations in frequency and duration of high and low flow pulses*

Hydrological pulses are the periods within a year in which the daily mean water condition either rises above 75th percentile (high pulses) or drops below the 25th percentile (low pulse) of all the daily values for the base period (Richter, 1996). Frequency of high pulses have increased in post-1990 period for stations Q465 and Q470 bygreater than 25 percent, however it has decreased at station Q460. High pulse duration though have decreased by 1.5 to 2 days in those stations. In case of low pulses, the count has increased in stations Q460 and Q470, but decreased in Q465. In station Q465, the low pulse duration has increased slightly by quarter day; but in remaining stations, it decreased by 1 to 3 days. Impact of alteration of changes in such pulses can be felt differently for different river systems and different causes of alteration. Xue et al. (2017) discusses the possibility of supply of nutrients to plants and animals at the river bank of Tarim River in China and development of river biodiversity because of increase of high pulse duration.

4.4.5. *Alterations in rate and frequency of flow conditions*

Parameter group 5 describes the alterations in the rate and frequency of flow conditions. Flow rise rate in station Q460 has increased after 1990 by about 10 percent; though in other stations it has decreased by 5 to 12 percent. However, the fall rate has decreased from about 8 to 13 at the three stations. Number of reversals in Q460 and in Q 465 has increased by about 54 percent and 11 percent; though it has decreased by about 5 percent at Q470. All the group 5 parameters at station Q470 have decreased, implying that the channel is undergoing more depositional process. Same is true for Q465 but since the reversal rate has increased, stabilization process may be slower than in case of Q470. Unlike these two stations, erosion processes may be more active in case of station Q460 with effects on overall annual stability of the river banks.

Table 5
Trends in the IHA parameters related to extremes at three gauging stations.

IHA parameters	Station	Mann-Kendall's Tau	p- value from M-MK test	Sen's slope (units / year)		p –value from Spearman rho test	Significance (α= 0.05) as per M-MK test	Significance (α= 0.05) per Spearman's rho test
1-day minimum flow (m^3/sec)	460	−0.178	0.234	−0.066	↓	0.319	NS	NS
	465	0.046	0.728	0.018	↑	0.889	NS	NS
	470	−0.145	0.133	−0.015	↓	0.360	NS	NS
7-day minimum flow (m^3/sec)	460	−0.159	0.286	−0.066	↓	0.407	NS	NS
	465	0.071	0.628	0.027	↑	0.708	NS	NS
	470	−0.071	0.319	−0.009	↓	0.673	NS	NS
30-day minimum flow (m^3/sec)	460	0.043	0.785	0.011	↑	0.668	NS	NS
	465	0.132	0.355	0.034	↑	0.403	NS	NS
	470	−0.025	0.803	−0.004	↓	0.848	NS	NS
1-day maximum flow (m^3/sec)	460	0.156	0.297	2.357	↑	0.339	NS	NS
	465	0.172	0.225	9.100	↑	0.173	NS	NS
	470	0.022	0.895	1.029	↑	0.841	NS	NS
7-day maximum flow (m^3/sec)	460	0.101	0.407	1.274	↑	0.471	NS	NS
	465	0.243	0.064	4.370	↑	0.084	NS	NS
	470	0.200	0.158	1.413	↑	0.226	NS	NS
30-day maximum flow (m^3/sec)	460	0.123	0.413	0.434	↑	0.521	NS	NS
	465	0.182	0.201	1.844	↑	0.204	NS	NS
	470	0.151	0.063	0.683	↑	0.279	NS	NS
Date of minimum flow (days)	460	0.228	0.124	1.142	↑	0.105	NS	NS
	465	0.175	0.217	1.588	↑	0.250	NS	NS
	470	−0.049	0.741	−0.467	↓	0.810	NS	NS
Date of maximum flow (days)	460	−0.167	0.18	−1.079	↓	0.267	NS	NS
	465	−0.295	NA	−1.800	↓	0.022	S	S
	470	−0.335	0.017	−2.000	↓	0.051	S	NS

Notes: Arrows ↑, and ↓ indicate increase and decrease in trends, respectively. 'S' and 'NS' are statistically significant & not significant.

Table 6
Timing of annual maximum and minimum extremes.

	Date of daily minimum flow (median) – n days from Jan 1			Date of daily maximum flow (median) – n days from Jan 1		
Station	Before 1990	After 1990	Changes	Before 1990	After 1990	Changes
460	109 (19 Apr)	134 (14 May)	25 (→)	246 (3 Sep)	220 (8 Aug)	26 (←)
465	77 (18 Mar)	105 (15 Apr)	28 (→)	243 (31 Aug)	210 (29 Jul)	33 (←)
470	121 (1 May)	126 (6 May)	5 (→)	247 (4 Sep)	214 (2 Aug)	33 (←)

Note: (a) Units are in days (b) → indicates delay or late shifting (c) ← indicates early shifting.

4.5. Inter-relationship between hydrological and climatic extremes

Hydrological extremes are the manifestation of the climatic extremes, specifically precipitation extremes. Stream flows are directly or indirectly proportional to the rainfall. Simple expression of this relationship is a rational formula, i.e., $Q = C \times I \times A$; where C is catchment coefficient, I is rainfall (intensity) and A is catchment area. It explicitly relates to the intensity of rainfall to the streamflow, i.e., extreme rainfalls should also result in the high discharge in stream. It implicitly relates the timing of flows in relation to the occurrence of rainfall, i.e., flow due to extreme rainfall events can be traced out in flow hydrograph and it depends upon the time of concentration of the catchment. Table 7 shows the relationship between high discharges at station Q460 (Rajaiya) (annual maximum flow as well as recorded floods) and the rainfall extremes (RX1day) occurring at rainfall stations upstream of Q460.

It is very clear from Table 7 that occurrence of annual maximum flows at Q460 are closely tied up with the occurrence of the extreme rainfall events. In addition, the flood record dates obtained from GoN (2020) and United Nations Office for Disaster Risk Reduction (2019) also can be seen associated with the RX1day rainfall. These are shown by the blue and green colours in the Table 7. For instance, in 2000, the flood recorded date is between period 30 July to 4 August, and three upstream rainfall stations (904 –Chisapani, 905- Daman and 925 – Rajaiya) have received rainfall of RX1day magnitude between the flood period. Likewise, in 2002, annual maximum flow occurred on 23 July as result of rainfall extremes (RX1day) in upstream on the same day. Table 7 also shows spatial variability of rainfall extremes in relationship to high flows and floods in the EER watershed. However, the regression analysis between the magnitude of annual maximum discharge and RX1day occurring on the same date (or day earlier) shows poor relationship in the watershed. This might be due to erroneous discharge reading for the high flows at the gauging station. For example, in observation records on 23-July 2002 and 9 July 2004, it can be seen that rainfall on the former date is approximately 2 times higher than the latter date but river flow is about 2.6 times lesser on the former date. Strong correlation between RX1day rainfall and corresponding flow as floods is shown by Basnyat et al. (2020) in the Bagmati basin, which is neighbouring basin to the east of the ERR watershed. The study showed that correlation coefficient between RX1day rainfall and flood discharge is approximately 0.74 with statistically significant results. As the Bagmati is located in the East of

Table 7
Annual maximum flows, floods and its relationship with extreme precipitation (RX1day).

Annual maximum flow		Flood date recorded (Only value of peak of hydrograph is given)		RX1day rainfall (mm)					Corresponding date of RX1day				
				904	905	906	919	925	904	905	906	919	925
Date	m^3/sec	Date	m^3/sec	Chisapani	Daman	Hetauda	Makwanpur Gadhi	Rajaiya	Chisapani	Daman	Hetauda	Makwanpur Gadhi	Rajaiya
29-Jun-00	917	30 Jul - 4 Aug 00	810	162	319	142	200	106	3-Aug-00	3-Aug-00	10-Jul-00	21-Sep-00	1-Aug-00
5-Sep-01	300	5-Sep-01	300	193	120	204	147	182	31-Jul-01	31-Jul-01	1-Aug-01	1-Aug-01	30-Jul-01
23-Jul-02	424	19-Aug-02	22	443	369	302	311	252	23-Jul-02	23-Jul-02	23-Jul-02	23-Jul-02	23-Jul-02
18-Aug-03	172	30 Jul - 2 Aug 03	144	344	129	457	298	156	18-Jul-03	31-Jul-03	31-Jul-03	31-Jul-03	30-Jul-03
9-Jul-04	1090	8-11 Jul 04	1090	156	168	270	391	52	11-Jul-04	11-Jul-04	11-Jul-04	10-Jul-04	9-Jul-04
7-Aug-05	348	25-27 Aug 05	178	220	90	187	162	199	27-Aug-05	7-Aug-05	27-Aug-05	27-Aug-05	7-Aug-05
9-Sep-06	536	DNA	DNA	35	71	175	160	209	11-Mar-06	9-Jun-06	9-Sep-06	25-Aug-06	9-Sep-06
17-Aug-07	569	DNA	DNA	104	170	207	162	114	17-Jul-07	20-Aug-07	17-Aug-07	12-Sep-07	16-Aug-07
23-Jul-08	281	DNA	DNA	56	39	85	80	82	2-Apr-08	31-Aug-08	15-Jun-08	25-Aug-08	19-Jun-08
5-Aug-09	582	5-10 Aug 09	582	102	101	171	146	136	6-Jul-09	27-Jul-09	6-Aug-09	1-Jul-09	31-Jul-09
24-Aug-10	1260	21-31 Aug 10	1260	77	85	239	71	126	23-Aug-10	24-Aug-10	24-Aug-10	11-Sep-10	24-Aug-10
27-Jul-11	652	DNA	DNA	136	100	148	160	112	1-Jul-11	31-May-11	2-Aug-11	2-Jul-11	1-Jul-11
3-Aug-12	613	DNA	DNA	87	57	186	181	84	3-Aug-12	24-Jun-12	3-Aug-12	19-Jul-12	19-Jul-12
11-Jul-13	297	2-Sep-13	148	136	95	188	66	96	16-Jun-13	16-Jun-13	10-Jul-13	3-Sep-13	10-Jul-13
14-Aug-14	569	29-Sep-14	59.3	137	91	110	71	66	15-Aug-14	15-Aug-14	24-Jul-14	4-Jul-14	15-Aug-14
30-Jul-15	167	DNA	DNA	55	43	142	81	47	21-Jun-15	16-Jul-15	30-Jul-15	18-Apr-15	21-Aug-15

EER, the similar relation can be expected for EER watershed as well, even though data has not shown it clearly, perhaps due to errors in data observation/recording for high floods. Since RX5day in most of the cases also includes day corresponding to RX1day, RX5day rainfall also have strong relationship with high flows and floods.

Precipitation extremes events like R95p, RX1day, RX5day, R20 are increasing in the ERR watershed as shown in Fig. 6. Simultaneously, hydrological extremes like 1-day maxima, 7 –day maxima and 30-day maxima are also increasing (Table 5). Likewise, the increase in the extremes like consecutive dry days is also affecting the minimum flows. This is a clear indication that increase in precipitation extremes are also causing increase in the hydrological variability in the ERR watershed.

In future, the precipitation extremes are projected to increase (IPCC, 2014). As explained in Section 4.2.3, precipitation extremes in the EER watershed are projected to increase even up to 40 percent. Sillmann et al. (2013b) estimates an increase of RX5day up to 20 percent in RCP 4.5 scenario and up to 50 percent in RCP 8.5 scenario during 2081–2100 for the South Asian region. Dhaubanjar et al. (2020), using projections of 19 different CORDEX-SA RCMs, projects prolonged monsoon effects and increase in the intense rain events in the Karnali region of the Western Nepal for both RCP scenarios. Similarly, another study (MoFE, 2019) projects an increase of very wet days (P95) by about 12 percent in 2036–2065 period for Chitwan and Makwanpur districts of the ERR watershed. Since, precipitation extremes are currently increasing and are projected to increase, its translation into extreme hydrological events are also expected in the ERR watershed.

5. Conclusions

Climatic and hydrological extremes are of greater concern to the socio-economy. Climatic extremes influence the impacts of water-induced disasters to the socio-economically vulnerable population. We examined the changes in temperature- and precipitation-based extremes in the Extended East Rapti (EER) watershed in the southern-central Nepal. We used ETCCDI indices for climate extremes and examined its trend in the base period 1980–2005. Besides, we presented the alterations in the river flow characteristics in pre- and post-1990 in the three sub-watersheds in the EER watershed. They were analysed using IHA indicators; and trend analysis were also performed in hydrological extreme indices. In order to assess the future changes in the climate extremes, we first selected a suitable ensemble out of 19 regional climate models (RCMs) using the Australian Climate Futures Framework based on changes in annual average precipitation and temperature changes in the three future time periods namely, near-future (2021–2045), mid-future (2046–2070) and far-future (2071–2095), as compared to the base period. Then, we computed the ETCCDI indices and analysed the changes.

Performance of bias correction: Ensemble spread of raw RCMs is large, indicating RCMs' limitations to fairly capture the extremes, even though ensemble means in some cases are closer to the observation as in CWD and TXx. RCMs model spread is higher at higher percentiles. Absolute value-based temperature indices are generally underestimated whereas count-based indices (e.g., TX90p, TN90p) are in agreement with observation. The spread of RCMs after bias correction are narrowed down and they match closely with observation for indices others than higher percentiles.

Projected changes in climate extreme magnitudes: The ERR watershed, like all the basins in Nepal, are highly influenced by the monsoon rainfall in JJAS season. Almost all of the heavy precipitation events occur in those months. Precipitation amount, dry days and heavy precipitation events are projected to increase in the future. Since, indices like R95p, RX1day and RX5day are closely associated with hydrological

extremes as floods and events like landslides, those events are also expected to increase together with precipitation extreme events. All the temperature-related extreme indices, in general, are projected to increase in future periods, in which increase is more pronounced under the RCP 8.5 scenario. Future, as projected by the RCMs for both scenarios, will be warmer with increase in temperature-based extreme indices like warm days (10–50%) and warm nights (15–60%), the daily maxima and minima based extremes (0.2–5.0 °C) and prolongation of warm spell duration. Projected increase in hotter days and nights together with the rise in extremes, and further coupled with other precipitation-related extremes, may result in compounded impacts to the societies and ecosystems.

Observed and projected trends in climatic extremes: Observed trends in precipitation extremes in the EER watershed for the baseline period (1980–2005) are clearly increasing over the years. Heavy rainfall amounts like maximum 1-day precipitation (RX1day), maximum consecutive 5-day precipitation (RX5day) and very wet day precipitation (R95p) are observed with increasing trends, though with varying rates and level of significance. Consecutive dry days (CDD) are increasing with simultaneous decrease in consecutive wet days (CWD). The numbers of heavy rainfall days (e.g. R20) are also increasing. In case of temperature-related extreme indices, they show mixed trends over the baseline period across the indices as well as stations. There is a clear indication of increase in warm nights and warm days, no change in warm spell duration; and mixed results for other indices. For example, TXx has increasing trends at two stations (s905 and s906), whereas trend in TNx is decreasing at stations 902 and 906. Similarly, TXn has decreasing trend at two stations (s902 and s905), and TNn has increasing trend at s902 and decreasing trend in s906. The trends, for both temperature- and precipitation-based extremes, vary spatially, mostly indicating same direction of trend albeit with varying magnitudes. Most of the projected climate extreme trends (e.g., TX90p, TN90p, R95p, RX5day) agree with the increasing observed trends during the baseline period, albeit with varying rates and different levels of significance.

Observed trends in hydrologic extremes: Alterations in the flow regime of rivers of the EER watershed is progressing. These alterations can be attributed to the anthropogenic changes in the EER watershed; especially after 1990 when lots of developments are underway inside the watershed. Trend analysis of different indicators shows they are not statistically significant, but they certainty provide us information on direction of alterations. For instance, extreme indicators of maximum flows are increasing in the ERR watershed. IHA indicators' shift from middle RVA category to high and low RVA categories in post-1990 period with medium and high degree of alterations show that variability is increasing in the rivers. Such increase of variability may have geomorphic and ecologic implications as described in (Richter et al. (1996)) and Graf (2006). Identification of geomorphic and ecological implications in river of the EER watershed requires a separate rigorous study.

Climate extremes, specially related to precipitation, have direct relation to the hydrological extremes and these can be seen in the watersheds of southern Nepal including the ERR watershed. We observe that both the precipitation and hydrological extremes are increasing in the watershed. Since, they bear direct relationship, future hydrological extremes mostly floods are expected to increase in future.

CRediT authorship contribution statement

Vishnu Prasad Pandey: Conceptualization, Funding acquisition, Investigation, Methodology, Project administration, Resources, Supervision, Visualization, Writing - original draft, Writing - review & editing. **Dibesh Shrestha:** Conceptualization, Data curation, Formal analysis, Investigation, Methodology, Software, Validation, Visualization, Writing - original draft, Writing - review & editing. **Mina Adhikari:** Conceptualization, Methodology, Supervision, Visualization, Writing - review & editing.

Declaration of Competing Interest

The authors declare that they have no known competing financial interests or personal relationships that could have appeared to influence the work reported in this paper.

Acknowledgements

International Development Research Center (IDRC) for funding this research through the project titled "Water-Induced Disaster Risk Management Planning in Nepal (grant number 108973-001)"; Ms. Sanita Dhaubanjar for preliminary pre-processing of raw hydro-meteorological data; Mr Rabin Sharma for supporting with exploring annual flood events; and Department of Hydrology and Meteorology for providing hydro-climatic data.

Annex A. . Description of the 19 RCMs considered in this study

ID	Short Name [GCM_RCM]	CORDEX South Asia RCM	Driving GCM	RCM Description	Contributing RCM Modeling Center	Timeframe	Coordinate
1	ACCESS_CCAM	CSIRO-CCAM-1391M	ACCESS1.0	Conformal Cubical Atmospheric Model – CCAM (Mcgregor and Dix, 2001)	Commonwealth Scientific and Industrial Research Organization (CSIRO), Marine and Atmospheric Research, Melbourne, Australia	Hist: 1970–2005 RCP4.5/8.5: 2006–2099	Regular
2	CanESM2_RegCM4	IITM-RegCM4	CCCma-CanESM2	The Abdus Salam International Centre for Theoretical Physics (ICTP) Regional Climatic Model version 4 - RegCM4 (Giorgi et al., 2012)	Centre for Climate Change Research (CCCR), Indian Institute of Tropical Meteorology (IITM), India	Hist: 1951–2005 RCP4.5/8.5: 2006–2099	Rotated_mercator
3	CNRM_CCAM	CSIRO-CCAM-1391M	CNRM-CM5	Conformal Cubical Atmospheric Model – CCAM (Mcgregor and Dix, 2001)	CSIRO, Marine and Atmospheric Research, Melbourne, Australia	Hist: 1970–2005 RCP4.5/8.5: 2006–2099	Regular
4	CNRM_RegCM4	IITM-RegCM4	CNRM-CM5	ICTP Regional Climatic Model version 4 - RegCM4 (Giorgi et al., 2012)	Centre for Climate Change Research (CCCR), IITM, India	Hist: 1951–2005 RCP4.5: 2006–2099	Rotated_mercator

(*continued on next page*)

(*continued*)

ID	Short Name [GCM_RCM]	CORDEX South Asia RCM	Driving GCM	RCM Description	Contributing RCM Modeling Center	Timeframe	Coordinate
						RCP8.5: 2006–2085	
5	CNRM_RCA4	SMHI-RCA4	CNRM-CM5	Rossby Centre regional atmospheric model version 4 - RCA4 (Samuelsson et al., 2011)	Rosssy Centre, Swedish Meteorological and Hydrological Institute (SMHI), Sweden	Hist: 1951–2005 RCP: 2006–2100	Rotated_pole
6	CSIRO_RegCM4	IITM-RegCM4	CSIRO-Mk3.6	ICTP Regional Climatic Model version 4 - RegCM4 (Giorgi et al., 2012)	Centre for Climate Change Research (CCCR), IITM, India	Hist: 1951–2005 RCP4.5/8.5: 2006–2099	Rotated_mercator
7	GFDL_CCAM	CSIRO-CCAM-1391M	GFDL-CM3	Conformal Cubical Atmospheric Model – CCAM (Mcgregor and Dix, 2001)	CSIRO, Marine and Atmospheric Research, Melbourne, Australia	Hist: 1970–2005 RCP4.5: 2006–2070 RCP8.5: 2006–2099	Regular
8	HadGEM_RA	HadGEM3-RA	HadGEM2-AO	HadGEM3 Regional Atmospheric Model (Moufouma-Okia and Jones, 2014)	Met Office Hadley Centre (MOHC), UK	Hist: 1970–2005 RCP4.5/8.5: 2006–2100	Curvilinear rotated_latitude_longitude
9	ICHEC_RCA4	SMHI-RCA4	ICHEC-EC-EARTH	Rossby Centre regional atmospheric model version 4 - RCA4 (Samuelsson et al., 2011)	Rosssy Centre, SMHI, Sweden	Hist: 1970–2005 RCP: 2006–2100	Curvilinear rotated_latitude_longitude
10	IPSLLR_RegCM4	IITM-RegCM4	IPSL-CM5A-LR	ICTP Regional Climatic Model version 4 - RegCM4 (Giorgi et al., 2012)	Centre for Climate Change Research (CCCR), IITM, India	Hist: 1951–2005 RCP4.5/8.5: 2006–2099	Rotated_mercator
11	IPSLMR_RCA4	SMHI-RCA4	IPSL-CM5A-MR	Rossby Centre regional atmospheric model version 4 - RCA4 (Samuelsson et al., 2011)	Rosssy Centre, SMHI, Sweden	Hist: 1951–2005 RCP: 2006–2100	Rotated_pole
12	MIROC5_RCA4	SMHI-RCA4	MIROC-MIROC5	Rossby Centre regional atmospheric model version 4 - RCA4 (Samuelsson et al., 2011)	Rosssy Centre, SMHI, Sweden	Hist: 1951–2005 RCP: 2006–2100	Rotated_pole
13	MPI_CCAM	CSIRO-CCAM-1391M	MPI-ESM-LR	Conformal Cubical Atmospheric Model – CCAM (Mcgregor and Dix, 2001)	CSIRO, Marine and Atmospheric Research, Melbourne, Australia	Hist: 1970–2005 RCP4.5/8.5: 2006–2099	Regular
14	MPI_REMO	MPI-CSC-REMO2009	MPI-ESM-LR	MPI Regional model 2009 -REMO2009 (Teichmann et al., 2013)	Climate Service Center (CSC), Germany	Hist: 1970–2005 RCP: 2006–2100	Regular
15	MPI_RCA4	SMHI-RCA4	MPI-ESM-LR	Rossby Centre regional atmospheric model version 4 - RCA4 (Samuelsson et al., 2011)	Rosssy Centre, SMHI, Sweden	Hist: 1951–2005 RCP: 2006–2100	Rotated_pole
16	MPIMR_RegCM4	IITM-RegCM4	MPI-ESM-MR	ICTP Regional Climatic Model version 4 - RegCM4 (Giorgi et al., 2012)	Centre for Climate Change Research (CCCR), IITM, India	Hist: 1951–2005 RCP4.5/8.5: 2006–2099	Rotated_mercator
17	NOAA_RegCM4	IITM-RegCM4	NOAA-GFDL-GFDL-ESM2M	ICTP Regional Climatic Model version 4 - RegCM4 (Giorgi et al., 2012)	Centre for Climate Change Research (CCCR), IITM, India	Hist: 1970–2005 RCP: 2006–2099	Curvilinear rotated_mercator
18	NOAA_RCA4	SMHI-RCA4	NOAA-GFDL-GFDL-ESM2M	Rossby Centre regional atmospheric model version 4 - RCA4 (Samuelsson et al., 2011)	Rosssy Centre, SMHI, Sweden	Hist: 1951–2005 RCP: 2006–2100	Rotated_pole
19	NorESM_CCAM	CSIRO-CCAM-1391M	NorESM-M	Conformal Cubical Atmospheric Model – CCAM (Mcgregor and Dix, 2001)	CSIRO, Marine and Atmospheric Research, Melbourne, Australia	Hist: 1970–2005 RCP4.5: 2006–2099 RCP8.5: None	Regular

Notes: All RCMs have spatial resolution of 0.44° X 0.44°. Hist. is historical; RCP is representative concentration pathways; GCM is global climate model; RCM is regional climate model.

Annex B. List of the regional climate models (RCMs) selected for consensus case in six climate future matrices.

	ID	RCM Name	Δpr (%)	Δtasmax (°C)	ID	RCM Name	Δpr (%)	Δtasmax (°C)
Near Future (NF)	RCP4.5 Scenario				RCP8.5 Scenario			
	1	ACCESS1_0-CSIRO-CCAM	−3.06	1.00	1	ACCESS1_0-CSIRO-CCAM	−3.65	1.22
	3	CNRM-CM5-CSIRO-CCAM	−5.71	0.74	2	CCCma-CanESM2_IITM-RegCM4	8.46	1.05
	4	CNRM-CM5_IITM-RegCM4	−5.12	0.72	3	CNRM-CM5-CSIRO-CCAM	−1.09	0.74
	5	CNRM-CM5_SMHI-RCA4	8.49	0.69	4	CNRM-CM5_IITM-RegCM4	−2.47	0.89
	6	CSIRO-Mk36_IITM-RegCM4	−3.99	1.65	6	CSIRO-Mk36_IITM-RegCM4	2.70	1.43
	7	GFDL-CM3-CSIRO-CCAM	−5.46	1.84	8	HadGEM3-RA	9.66	1.39
	8	HadGEM3-RA	7.70	1.09	10	IPSL-CM5A-LR_IITM-RegCM4	4.00	0.96
	9	ICHEC-EC-EARTH-SMHI-RCA4	7.61	0.81	12	MIROC-MIROC5_SMHI-RCA4	4.30	1.35
	10	IPSL-CM5A-LR_IITM-RegCM4	−0.53	0.92	13	MPI-ESM-LR-CSIRO-CCAM	1.67	1.08
	11	IPSL-CM5A-MR_SMHI-RCA4	4.01	1.50	14	MPI-ESM-LR-MPI-CSC-REMO2009	−1.02	1.68
	13	MPI-ESM-LR-CSIRO-CCAM	−2.44	0.75	15	MPI-ESM-LR_SMHI-RCA4	7.96	1.40
	14	MPI-ESM-LR-MPI-CSC-REMO2009	−5.37	1.51	17	NOAA-GFDL-GFDL-ESM2M-IITM-RegCM4	−0.21	1.21
	16	MPI-ESM-MR_IITM-RegCM4	−3.05	0.83				
	17	NOAA-GFDL-GFDL-ESM2M-IITM-RegCM4	1.74	1.08				
	19	NorESM1-M-CSIRO-CCAM	−4.72	0.83				
Mid-Future (MF)	1	ACCESS1_0-CSIRO-CCAM	2.32	1.47	1	ACCESS1_0-CSIRO-CCAM	−2.19	2.61
	2	CCCma-CanESM2_IITM-RegCM4	7.58	1.42	11	IPSL-CM5A-MR_SMHI-RCA4	6.23	2.98
	3	CNRM-CM5-CSIRO-CCAM	2.57	0.73	12	MIROC-MIROC5_SMHI-RCA4	−3.22	2.44
	4	CNRM-CM5_IITM-RegCM4	−3.51	1.19	13	MPI-ESM-LR-CSIRO-CCAM	7.70	2.07
	9	ICHEC-EC-EARTH-SMHI-RCA4	7.68	1.63	15	MPI-ESM-LR_SMHI-RCA4	−1.39	2.72
	12	MIROC-MIROC5_SMHI-RCA4	5.50	1.63	16	MPI-ESM-MR_IITM-RegCM4	−4.44	2.20
	13	MPI-ESM-LR-CSIRO-CCAM	−0.06	1.32	17	NOAA-GFDL-GFDL-ESM2M-IITM-RegCM4	0.78	2.13
	15	MPI-ESM-LR_SMHI-RCA4	−0.25	1.98				
	16	MPI-ESM-MR_IITM-RegCM4	−7.33	1.63				
	17	NOAA-GFDL-GFDL-ESM2M-IITM-RegCM4	3.80	1.48				
	18	NOAA-GFDL-GFDL-ESM2M_SMHI-RCA4	−9.26	1.77				
	19	NorESM1-M-CSIRO-CCAM	2.07	0.98				
Far Future (FF)	2	CCCma-CanESM2_IITM-RegCM4	8.03	1.62	2	CCCma-CanESM2_IITM-RegCM4	9.61	2.88
	3	CNRM-CM5-CSIRO-CCAM	−1.17	1.32	3	CNRM-CM5-CSIRO-CCAM	0.93	3.04
	4	CNRM-CM5_IITM-RegCM4	−0.29	1.25	17	NOAA-GFDL-GFDL-ESM2M-IITM-RegCM4	5.35	3.07
	9	ICHEC-EC-EARTH-SMHI-RCA4	7.95	1.86	18	NOAA-GFDL-GFDL-ESM2M_SMHI-RCA4	0.74	3.44
	13	MPI-ESM-LR-CSIRO-CCAM	3.59	1.42				
	16	MPI-ESM-MR_IITM-RegCM4	−9.10	1.58				
	17	NOAA-GFDL-GFDL-ESM2M-IITM-RegCM4	4.94	1.67				
	19	NorESM1-M-CSIRO-CCAM	1.62	1.41				

Notes: ID corresponds to identification number of Regional Climate Model (RCM) in Annex-A; Δpr change in precipitation; Δtasmax is change in average temperature.

References

Abebe, W.B., Tilahun, S.A., Moges, M.M., Wondie, A., Derseh, M.G., Nigatu, T.A., Mhiret, D.A., Steenhuis, T.S., Camp, M.V., Walraevens, K., McClain, M.E., 2020. Hydrological foundation as a basis for a holistic environmental flow assessment of tropical highland rivers in Ethiopia. Water 12 (2), 547. https://doi.org/10.3390/w12020547.

Alexander, V., Zhang, X., Peterson, T.C., Caesar, J., Gleason, B., Tank, A.M.G.K., Vincent, L., 2006. Global observed changes in daily climate extremes of temperature and precipitation. J. Geophys. Res. 111, D05109. https://doi.org/10.1029/2005JD006290.

Baidya, S.K., Shrestha, M.L., Sheikh, M.M., 2008. Trends in daily climatic extremes of temperature and precipitation in Nepal. J. Hydrol. Meteorol. 5 (1), 38–51.

Basnyat, D.B., Shrestha, D., Thapa, S., Bajimaya, S., Maharjan, M., Shrestha, S., Dhungana, S., 2020. Post-flood assessment of the 2019 flooding in the Bagmati River Basin, Nepal. J. Dev. Innov. 4 (1), 20–47.

Bates, B., Kundzewicz, Z., Wu, S., Palutikof, J., 2008. Climate Change and Water. Technical Paper of the Intergovernmental Panel on Climate Change, IPCC Secretariat, Geneva, p. 210.

Bharati, L., Gurung, P., Maharjan, L., Bhattarai, U., 2016. Past and future variability in the hydrological regime of the Koshi Basin, Nepal. Hydrol. Sci. J. 61 (1), 79–93. https://doi.org/10.1080/02626667.2014.95263.

Berckmans, J., Hamdi, R., Dendoncker, N., 2019. Bridging the gap between policy-driven land use changes and regional climate projections. J. Geophys. Res. Atmos. 124 (12), 5934–5950. https://doi.org/10.1029/2018JD029207.

Clarke JM, Whetton PH, Hennessy KJ., 2011. Providing Application-specific Climate Projections Datasets: CSIRO's Climate Futures Framework. MODSIM2011, 19th Int Congr Model Simul 2683–2687. doi: 10.13140/2.1.1915.2649.

Dery, S.J., Stadnyk, T.A., Macdonald, M.K., Gauli-sharma, B., 2016. Recent trends and variability in river discharge across northern Canada. Hydrol. Earth Syst. Sci. 20, 4801–4818. https://doi.org/10.5194/hess-20-4801-2016.

Devkota, L.P., Gyawali, D.R., 2015. Impacts of climate change on hydrological regime and water resources management of the Koshi River Basin, Nepal. J. Hydrol. Reg. Stud. 4, 502–515. https://doi.org/10.1016/j.ejrh.2015.06.023.

Dhaubanjar, S., Pandey, V.P., Bharati, L., 2020. Climate futures for Western Nepal based on regional climate models in the CORDEX-SA. Int. J. Climatol. 40 (4), 2201–2225. https://doi.org/10.1002/joc.6327.

Donat, M., Alexander, L., Yang, H., Durre, I., Vose, R., Dunn, R., Willett, K., Aguilar, E., Brunet, M., Caesar, J., 2013. Updated analyses of temperature and precipitation extreme indices since the beginning of the twentieth century: the HadEX2 dataset. J. Geophys. Res.: Atmos. 118, 2098–2118. https://doi.org/10.1002/jgrd.50150.

Enayati, M., Bozorg-Haddad, O., Bazrafshan, J., Hejabi, S., Chu, X., 2020. Bias correction capabilities of quantile mapping methods for rainfall and temperature variables. J. Water Clim. Change. https://doi.org/10.2166/wcc.2020.261.

Gaur, S., Bandyopadhyay, A., Singh, R., 2020. Modelling potential impact of climate change and uncertainty on streamflow projections: a case study. J. Water Clim. Change, In Press. https://doi.org/10.2166/wcc.2020.254.

GoN, 2020. Nepal Disaster Risk Reduction Portal. Government of Nepal (GoN). Retrieved from http://drrportal.gov.np/ (on 15th July, 2020).

Giorgi, F., Coppola, E., Solmon, F., et al., 2012. RegCM4: Model description and preliminary tests over multiple CORDEX domains. Climate Research 52, 7–29. https://doi.org/10.3354/cr01018.

Graf, W.L., 2006. Downstream hydrologic and geomorphic effects of large dams on American rivers. Geomorphology 79 (3–4), 336–360.

Gudmundsson, L., Bremnes, J.B., Haugen, J.E., Engen-Skaugen, T., 2012. Downscaling RCM precipitation to the station scale using statistical transformations–a comparison of methods. Hydrol. Earth Syst. Sci. 16 (9), 3383–3390.

Gutowski Jr, W.J., Ullrich, P.A., Hall, A., Leung, L.R., O'Brien, T.A., Patricola, C.M., Arritt, R.W., Bukovsky, M.S., Calvin, K.V., Feng, Z., Jones, A.D., Kooperman, G.J.,

Monier, E., Pritchard, M.S., Pryor, S.C., Qian, Y., Rhoades, A.M., Roberts, A.F., Sakaguchi, K., Urban, N., Zarzycki, C., 2020. The ongoing need for high-resolution regional climate models: process understanding and stakeholder information. Bull. Am. Meteorol. Soc. 101 (5), E664–E683.

HI-AWARE, 2017. The Gandaki Basin Maintaining Livelihood in the Face of Landslides, Floods and Drought. HI-AWARE Working Paper 9, ICIMOD, Nepal.

Hamed, K.H., Rao, A.R., 1998. A modified Mann-Kendall trend test for autocorrelated data. J. Hydrol. 204 (1–4), 182–196. https://doi.org/10.1016/s0022-1694(97)00125-x.

Hirsch, R.M., Slack, J.R., Smith, R.A., 1982. Techniques of trend analysis for monthly water quality data. Water Resour. Res. 18 (1), 10712. https://doi.org/10.1029/wr018i001p00107.

ICIMOD, 2010. Land Cover of Nepal 2010. International Center for Integrated Mountain Development (ICIMOD), Kathmandu, Nepal. Available online at: http://rds.icimod.org/Home/DataDetail?metadataId=9224 [Accessed on 12thJanuary 2017).

ICIMOD, 2017. Status of Gender, Vulnerabilities and Adaptation to Climate Change in the Hindu Kush Himalaya, Impact and Implication for Livelihood and Sustainable Mountain Development (ICIMOD). ICIMOD, Kathmandu.

IPCC, 2014. Summary for policymakers. In: Climate Change 2014: Impacts, Adaptation, and Vulnerability. Part A: Global and Sectoral Aspects. Contribution of Working Group II to the Fifth Assessment Report of the Intergovernmental Panel on Climate Change [Field, C.B., V.R. Barros, D.J. Dokken, K.J. Mach, M.D. Mastrandrea, T. E. Bilir, M. Chatterjee, K.L. Ebi, Y.O. Estrada, R.C. Genova, B. Girma, E.S. Kissel, A.N. Levy, S. MacCracken, P.R. Mastrandrea, and L.L. White (eds.)]. Cambridge University Press, Cambridge, United Kingdom and New York, NY, USA, pp. 1-32.

Islam, Md N., 2009. Understanding the rainfall climatology and detection of extreme weather events in the SAARC region: Part II-Utilization of RCM data, SMRC – No. 29. SAARC Meteorological Research Centre (SMRC) E-4/C, Agargaon, Dhaka-1207, Bangladesh.

Jacob, D., Teichmann, C., Sobolowski, S. et al., 2020. Regional climate downscaling over Europe: perspectives from the EURO-CORDEX community. Reg Environ Change 20, 51 (2020). https://doi.org/10.1007/s10113-020-01606-9.

Karki, R., Schickhoff, U., Scholten, T., Böhner, J., 2017. Rising precipitation extremes across Nepal. Climate 5 (1), 4. https://doi.org/10.3390/cli5010004.

Kendall, M.G., 1975. Rank Correlation Methods, 4th ed. Charles Griffin, London.

Khatiwada, K.R., Panthi, J., Shrestha, M.L., 2016. Hydro-climatic variability in the Karnali River Basin of Nepal Himalaya. Climate 4 (17), 1–15. https://doi.org/10.3390/cli4020017.

Kiktev, D., Sexton, D.M.H., Alexander, L., Folland, C.K., 2003. Comparison of modeled and observed trends in indices of daily climate extremes. J. Clim. 16, 3560–3571.

Kundzewicz, Z.W., Merz, B., Vorogushyn, S., Hartmann, H., Duethmann, D., Wortmann, M., Krysanova, V., 2015. Analysis of changes in climate and river discharge with focus on seasonal runoff predictability in the Aksu River Basin. Environ. Earth Sci. 73, 501–516. https://doi.org/10.1007/s12665-014-3137-5.

Lamichhane, S., Shakya, N.M., 2019. Integrated assessment of climate change and land use change impacts on hydrology in the Kathmandu Valley Watershed. Central Nepal. Water 11 (10), 2059. https://doi.org/10.3390/w11102059.

Lehmann, E.L., 1975. Nonparametrics: statistical methods based on ranks. Holden-Day Inc, California, p. 457.

Mann, H.B., 1945. Non-parametric tests against trend. Econometrica 13, 245–249.

Mathews, R., Richter, B.D., 2007. Application of the Indicators of hydrologic alteration software in environmental flow setting 1. JAWRA J. Am. Water Resour. Assoc. 43 (6), 1400–1413.

MoFE, 2019. Climate change scenarios for Nepal for National Adaptation Plan (NAP). Ministry of Forests and Environment (MoFE), Kathmandu.

Mcgregor, J.L., Dix, M.R., 2001. The CSIRO Conformal-Cubic Atmospheric GCM. In: Hodnett, P.F. (Ed.), Fluid Mechanics and Its Applications, 61. Springer, Dordrecht, pp. 197–202. https://doi.org/10.1007/978-94-010-0792-4_25.

MoHA/GoN, 2015. Disaster Data 2068 to 2071 (2011 to 2014). Ministry of Home Affairs, Government of Nepal (MoHA/GoN). Available online at https://bit.ly/2PVsv1d.

MoHA/GoN, 2017. Disaster Risk Management in Nepal: Status, Achievements. Challenges and Ways Forward, Ministry of Home Affairs, Government of Nepal (MoHA/GoN). Available at http://bit.ly/2CSk2cr.

MoSTE, 2014. Economic Impact Assessment of Climate Change in Key Sectors in Nepal. The Government of Nepal, Ministry of Science, Technology and Environment (MoSTE).

OCHA, 2008. Nepal: Koshi River flood in Sunsari and Saptari UN Office for the Coordination of Humanitarian Affairs (OCHA), Situation Report No.9., Kathmandu.

Moufouma-Okia, W., Jones, R., 2014. Resolution dependence in simulating the African hydroclimate with the HadGEM3-RA regional climate model. Climate Dynamics 44, 609–632. https://doi.org/10.1007/s00382-014-2322-2.

Panda, D.K., Kumar, A., Ghosh, A., Mohanty, R.K., 2013. Streamflow trends in the Mahanadi River basin (India): linkages to tropical climate variability. J. Hydrol. 495, 135–149.

Pandey, V.P., Dhaubanjar, S., Bharati, L., Thapa, B.R., 2019. Hydrological response of Chamelia watershed in Mahakali Basin to climate change. Sci. Total Environ. 650, 365–383. https://doi.org/10.1016/j.scitotenv.2018.09.053.

Pandey, V.P., Dhaubanjar, S., Bharati, L., Thapa, B.R., 2020a. Spatio-temporal distribution of water availability in Karnali-Mohana basin, Western Nepal: climate change impact assessment (Part-B). J. Hydrol.: Reg. Stud. 29, 100690.

Pandey, V.P., Shrestha, D., Adhikari, M., Shakya, S., 2020b. Streamflow alterations, attributions, and implications in extended East Rapti Watershed, Central-Southern Nepal. Sustainability 12 (9), 3829.

Pokharel, A.K., Hallett, J., 2015. Distribution of rainfall intensity during the summer monsoon season over Kathmandu, Nepal. Weather 70 (9), 257–261. https://doi.org/10.1002/wea.2544.

Ray, A., 2020. Assessment of climate change impacts on water sufficiency and gender mainstreaming in the Extended East Rapti watershed, Nepal. Master of Engineering in Interdisciplinary Water Resources Management. Nepal Engineering College, Pokhara University, Nepal.

Rijal, K.P., 2015. Climate change and its impact on rice yield. Hydro Nepal 16, 23–27.

Richter, B., Baumgartner, J., Wigington, R., Braun, D., 1997. How much water does a river need? Freshw. Biol. 37 (1), 231–249.

Richter, B.D., Baumgartner, J.V., Powell, J., Braun, D.P., 1996. A method for assessing hydrologic alteration within ecosystems. Conserv. Biol. 10 (4), 1163–1174.

Samuelsson, P., Jones, C.G., Willén, U., et al., 2011. The Rossby Centre Regional Climate model RCA3: model description and performance. Tellus A 63 (1), 4–23. https://doi.org/10.1111/j.1600-0870.2010.00478.x.

Sanjay, J., Krishnan, R., Shrestha, A.B., Rajbhandari, R., Ren, G.Y., 2017. Downscaled climate change projections for the Hindu Kush Himalayan region using CORDEX South Asia regional climate models. Adv. Clim. Change Res. 8 (3), 185–198.

Sen, P.K., 1968. Estimates of the regression coefficient based on Kendall's Tau. J. Am. Stat. Assoc. 63 (324), 1379–1389. https://doi.org/10.1080/01621459.1968.10480934.

Seneviratne, S.I., N. Nicholls, D. Easterling, C.M. Goodess, S. Kanae, J. Kossin, Y. Luo, J. Marengo, K. McInnes, M. Rahimi, M. Reichstein, A. Sorteberg, C. Vera, and X. Zhang, 2012: Changes in climate extremes and their impacts on the natural physical environment. In: Managing the Risks of Extreme Events and Disasters to Advance Climate Change Adaptation [Field, C.B., V. Barros, T.F. Stocker, D. Qin, D.J. Dokken, K.L. Ebi, M.D. Mastrandrea, K.J. Mach, G.-K. Plattner, S.K. Allen, M. Tignor, and P.M. Midgley (eds.)]. A Special Report of Working Groups I and II of the Intergovernmental Panel on Climate Change (IPCC). Cambridge University Press, Cambridge, UK, and New York, NY, USA, pp. 109-230.

Sharmila, S., Joseph, S., Sahai, A.K., Abhilash, S., Chattopadhyay, R., 2015. Future projection of Indian summer monsoon variability under climate change scenario: An assessment from CMIP5 climate models. Global Planet. Change 124, 62–78.

Shrestha, M., Acharya, S.C., Shrestha, P.K., 2017. Bias correction of climate models for hydrological modelling – are simple methods still useful? Meteorol. Appl. 24 (3), 531–539. https://doi.org/10.1002/met.1655.

Sillmann, J., Kharin, V.V., Zhang, X., Zwiers, F.W., Bronaugh, D., 2013a. Climate extremes indices in the CMIP5 multimodel ensemble: Part 1. Model evaluation in the present climate. J. Geophys. Res.: Atmos. 118 (4), 1716–1733.

Sillmann, J., Kharin, V.V., Zwiers, F.W., Zhang, X., Bronaugh, D., 2013b. Climate extremes indices in the CMIP5 multimodel ensemble: Part 2. Future climate projections. J. Geophys. Res.: Atmos. 118 (6), 2473–2493.

Singh, D., Ghosh, S., Roxy, M.K., McDermid, S., 2019. Indian summer monsoon: Extreme events, historical changes, and role of anthropogenic forcings. Wiley Interdiscip. Rev. Clim. Change 10 (2), e571.

Sneyers, S., 1990. On the statistical analysis of series of observations. Technical note No. 143, WMO No 415. World Meteorological Organization, Geneva, pp:192.

Stefanidis, S., Dafis, S., Stathis, D., 2020. Evaluation of regional climate models (RCMs) performance in simulating seasonal precipitation over mountainous Central Pindus (Greece). Water 12, 2750. https://doi.org/10.3390/w12102750.

Suman, M., Maity, R., 2020. Southward shift of precipitation extremes over south Asia: evidences from CORDEX data. Sci. Rep. 10 (1), 1–11.

Talchabhadel, R., Karki, R., Thapa, B.R., Maharjan, M., Parajuli, B., 2018. Spatio-temporal variability of extreme precipitation in Nepal. Int. J. Climatol. https://doi.org/10.1002/joc.5669.

Teichmann, C., Eggert, B., Elizalde, A., et al., 2013. How Does a Regional Climate Model Modify the Projected Climate Change Signal of the Driving GCM: A Study over Different CORDEX Regions Using REMO. Atmosphere 4 (2), 214–236. https://doi.org/10.3390/atmos4020214.

Teutschbein, C., Seibert, J., 2012. Bias correction of regional climate model simulations for hydrological climate-change impact studies: Review and evaluation of different methods. J. Hydrol. 456, 12–29.

Themeßl, M.J., Gobiet, A., Heinrich, G., 2012. Empirical-statistical downscaling and error correction of regional climate models and its impact on the climate change signal. Clim. Change 112 (2), 449–468.

The Nature Conservancy, 2009. Indicators of hydrologic alteration, version 7.1. User's Manual. The Nature Conservancy, Charlottesville, Virginia.

United Nations Office for Disaster Risk Reduction, 2019. DesInventar as a Disaster Information Management System. Retrieved from https://www.desinventar.net/ (16th July, 2020).

Whetton, P., Hennessy, K., Clarke, J., et al., 2012. Use of Representative Climate Futures in impact and adaptation assessment. Clim. Change 115, 433–442. https://doi.org/10.1007/s10584-012-0471-z.

WMO, 2009. Guidelines on analysis of extremes in a changing climate in support of informed decisions for adaptation. WCDMP 72, World Meteorological Organization, Geneva.

Xue, L., Zhang, H., Yang, C., Zhang, L., Sun, C., 2017. Quantitative assessment of hydrological alteration caused by irrigation projects in the Tarim River basin. China. Sci. Rep. 7 (4291), 1–13. https://doi.org/10.1038/s41598-017-04583-y.

Zeiringer, B., Seliger, C., Greimel, F., Schmutz, S., 2018. River hydrology, flow alteration, and environmental flow. In: Riverine Ecosystem Management. Springer, Cham, pp. 67–89.

Zhang, X., Feng, Y., Chan, R., 2018. User's manual: Introduction to RClimDex v1.9 Climate Research Division Environment Canada Downsview, Ontario Canada December 12, 2018.